



HAL
open science

**Introduction of organic/hydro-organic matrices in
inductively coupled plasma optical emission
spectrometry and mass spectrometry: A tutorial review.
Part I. Theoretical considerations**

Amélie Leclercq, Anthony Nonell, José Luis Todolí Torró, Carole Bresson,
Laurent Vio, Thomas Vercouter, Frédéric Chartier

► **To cite this version:**

Amélie Leclercq, Anthony Nonell, José Luis Todolí Torró, Carole Bresson, Laurent Vio, et al.. Introduction of organic/hydro-organic matrices in inductively coupled plasma optical emission spectrometry and mass spectrometry: A tutorial review. Part I. Theoretical considerations. *Analytica Chimica Acta*, 2015, 885, pp.33-56. 10.1016/j.aca.2015.03.049 . cea-03188933

HAL Id: cea-03188933

<https://cea.hal.science/cea-03188933>

Submitted on 12 Mar 2024

HAL is a multi-disciplinary open access archive for the deposit and dissemination of scientific research documents, whether they are published or not. The documents may come from teaching and research institutions in France or abroad, or from public or private research centers.

L'archive ouverte pluridisciplinaire **HAL**, est destinée au dépôt et à la diffusion de documents scientifiques de niveau recherche, publiés ou non, émanant des établissements d'enseignement et de recherche français ou étrangers, des laboratoires publics ou privés.

Accepted Manuscript

Title: Introduction of organic/hydro-organic matrices in inductively coupled plasma optical emission spectrometry and mass spectrometry: a tutorial review. Part I. Theoretical considerations

Author: Amélie Leclercq Anthony Nonell José Luis Todolí Torró Carole Bresson Laurent Vio Thomas Vercouter Frédéric Chartier



PII: S0003-2670(15)00440-7
DOI: <http://dx.doi.org/doi:10.1016/j.aca.2015.03.049>
Reference: ACA 233835

To appear in: *Analytica Chimica Acta*

Received date: 5-11-2014
Revised date: 20-2-2015
Accepted date: 27-3-2015

Please cite this article as: Amélie Leclercq, Anthony Nonell, José Luis Todolí Torró, Carole Bresson, Laurent Vio, Thomas Vercouter, Frédéric Chartier, Introduction of organic/hydro-organic matrices in inductively coupled plasma optical emission spectrometry and mass spectrometry: a tutorial review. Part I. Theoretical considerations, *Analytica Chimica Acta* <http://dx.doi.org/10.1016/j.aca.2015.03.049>

This is a PDF file of an unedited manuscript that has been accepted for publication. As a service to our customers we are providing this early version of the manuscript. The manuscript will undergo copyediting, typesetting, and review of the resulting proof before it is published in its final form. Please note that during the production process errors may be discovered which could affect the content, and all legal disclaimers that apply to the journal pertain.

Introduction of organic/hydro-organic matrices in inductively coupled plasma optical emission spectrometry and mass spectrometry: a tutorial review. Part I. Theoretical considerations

**Amélie Leclercq¹, Anthony Nonell¹, José Luis Todolí Torró², Carole Bresson¹, Laurent Vio¹,
Thomas Vercouter¹, Frédéric Chartier³**

¹CEA Saclay, DEN, DANS, DPC, SEARS, Laboratoire de développement Analytique Nucléaire
Isotopique et Élémentaire, 91191 Gif-sur-Yvette, France

amelie.leclercq@cea.fr, anthony.nonell@cea.fr, carole.bresson@cea.fr, laurent.vio@cea.fr,
thomas.vercouter@cea.fr

²Universidad de Alicante, Departamento de Química Analítica, Nutrición y Bromatología, Ap.
de Correos, 99, 03080 Alicante, Spain, jose.todoli@ua.es

³CEA Saclay, DEN, DANS, DPC, 91191 Gif-sur-Yvette, France, frederic.chartier@cea.fr

Corresponding authors:

Amélie Leclercq, tel: +33(0)1 69 08 18 47, fax: +33(0)1 69 08 54 11, amelie.leclercq@cea.fr

Anthony Nonell, tel: +33(0)1 69 08 32 51, fax: +33(0)1 69 08 54 11, anthony.nonell@cea.fr

Graphical abstract

Highlights

Tutorial review addressed to beginners or more experienced analysts

Theoretical background of effects caused by organic matrices on ICP techniques

Spatial distribution of carbon species and analytes in plasma

Carbon spectroscopic and non-spectroscopic interferences in ICP

Keywords: inductively coupled plasma, mass spectrometry, optical emission spectrometry, organic matrices, carbon constituents, interferences

Abstract

Due to their outstanding analytical performances, inductively coupled plasma optical emission spectrometry (ICP-OES) and mass spectrometry (ICP-MS) are widely used for multi-elemental measurements and also for isotopic characterization in the case of ICP-MS. While most studies are carried out in aqueous matrices, applications involving organic/hydro-organic matrices become increasingly widespread. This kind of matrices is introduced in ICP based instruments when classical "matrix removal" approaches such as acid digestion or extraction procedures cannot be implemented. Due to the physico-chemical properties of organic/hydro-organic matrices and their associated effects on instrumentation and analytical performances, their introduction into ICP sources is particularly challenging and has become a full topic. In this framework, numerous theoretical and phenomenological studies of these effects have been performed in the past, mainly by ICP-OES, while recent literature

is more focused on applications and associated instrumental developments. This tutorial review, divided in two parts, explores the rich literature related to the introduction of organic/hydro-organic matrices in ICP-OES and ICP-MS. The present Part I, provides theoretical considerations in connection with the physico-chemical properties of organic/hydro-organic matrices, in order to better understand the induced phenomena. This focal point is divided in four chapters highlighting: (i) the impact of organic/hydro-organic matrices from aerosol generation to atomization/excitation/ionization processes; (ii) the production of carbon molecular constituents and their spatial distribution in the plasma with respect to analytes repartition; (iii) the subsequent modifications of plasma fundamental properties; and, (iv) the resulting spectroscopic and non spectroscopic interferences. This first part of this tutorial review is addressed either to beginners or to more experienced scientists who are interested in the analysis of organic/hydro-organic matrices by ICP sources and would like to consider the theoretical background of effects induced by such matrices.

The second part of this tutorial review will be dedicated to more practical consideration on instrumentation, such as adapted introduction devices, as well as instrumental and operating parameters optimization. The analytical strategies for elemental quantification in such matrices will also be addressed.

Glossary of terms	
$D_{3,2}$	Sauter mean diameter (μm)
ICP	inductively coupled plasma
ICP-AES	inductively coupled plasma atomic emission spectroscopy
ICP-MS	inductively coupled plasma mass spectrometry
ICP-OES	inductively coupled plasma optical emission spectrometry
RF	radio frequency (MHz)
S_{tot}	total mass solvent transport rate (mg min^{-1} or $\mu\text{g s}^{-1}$)
W_{tot}	total mass analyte transport rate ($\mu\text{g min}^{-1}$ or $\mu\text{g s}^{-1}$)

Summary

1. Introduction	6
2. Physico-chemical properties of organic solvents and associated effects on ICP-OES and ICP-MS stages	8
2.1. Definitions and classifications.....	8
2.2. Impacts of organic/hydro-organic matrices on ICP-OES and ICP-MS stages: from aerosol generation to atomization/excitation/ionization processes	10
2.3. Plasma tolerance and robustness.....	17
3. Molecular constituents in the plasma and their spatial distribution	22
3.1. Main constituents	22
3.2. Spatial distribution of carbon species	23
3.3. Spatial distribution of analytes	25
4. Impact of organic/hydro-organic matrices on plasma fundamental properties	27
4.1. Excitation temperature	27
4.2. Electron number density	29
4.3. Carbon deposition.....	30
5. Spectroscopic and non-spectroscopic interferences	31
5.1. Spectroscopic interferences	31
5.2. Non-spectroscopic interferences.....	33
6. Conclusion	36
Figures	59
Tables	68
References	Error! Bookmark not defined.

1. Introduction

Inductively coupled plasma (ICP) techniques, particularly renowned for their sensitivity and selectivity [1], are the most widely used for trace-element measurements [2]. Three ICP technologies have been developed: optical emission spectrometry (ICP-OES, also called atomic emission spectroscopy, ICP-AES), mass spectrometry (ICP-MS) [1, 3] and to a lesser extent atomic fluorescence spectrometry (ICP-AFS). ICP sources allow the atomization and the almost complete ionization of all elements in a wide range of samples [4]. Therefore, ICP-OES and ICP-MS techniques have been widely used over the years in various fields of applications, to carry out multi-elemental analyses and also isotopic characterizations in the case of ICP-MS (Figure 1) [1, 5].

Most of the ICP studies are performed in aqueous mode. However, applications involving organic/hydro-organic matrices have considerably grown over the past years in many fields, including petroleum industry, biology, environment, etc. (Figure 2). Therefore, the introduction of this kind of matrices into ICP sources, *via* direct introduction or following a separation step, has become a full topic that deserves going further into consideration. Pure organic or hydro-organic matrices can be distributed following the classification proposed by Todolí and Mermet, according to [6]: (i) samples of organic nature, *e.g.* petroleum products (*e.g.* [7-11]); (ii) samples treated with organic solvents such as dissolution or analyte extractions (*e.g.* [12-15]); (iii) high-viscosity samples requiring dilution in organic solvents or micro-emulsion (*e.g.* [15-18]); and (iv) samples in mobile phases coming from separation techniques (*e.g.* [19-32]).

Organic/hydro-organic matrices introduction into ICP sources remains challenging, due to their variable impacts at each stage of the instrumentation: sample introduction,

nebulization, aerosol transport, atomization/excitation/ionization steps, ions extraction, etc. The multiplicity of samples/matrices with different associated physico-chemical properties renders the task much more difficult.

Although ICP has been the subject of many books and reviews (e.g. [4, 5, 10, 11, 33-56]), only few of these, principally focused on petroleum applications, deal with the introduction of organic/hydro-organic matrices [10, 11, 55, 56]. In addition, diverse liquid samples introduction devices have been recently reviewed, including some considerations inorganic/hydro-organic matrices properties [6].

The first part of this tutorial review is addressed either to beginners or to more experienced scientists who are interested in the analysis of organic/hydro-organic matrices with ICP sources and would like to consider the theoretical background about the effects induced by such matrices. The aim of this part is to comprehensively explore the literature concerning theoretical considerations on (i) the impact of organic/hydro-organic matrices from aerosol generation to atomization/excitation/ionization processes; (ii) the production of carbon molecular constituents and their spatial distribution in the plasma with respect to analytes repartition; (iii) the subsequent modifications of plasma fundamental properties; and, (iv) the resulting spectroscopic and non spectroscopic interferences.

The second part of this tutorial review will be dedicated to more practical considerations on instrumentation, such as adapted introduction devices, as well as instrumental and operating parameters optimization. The analytical strategies for elemental quantification in such matrices will also be addressed.

2. Physico-chemical properties of organic solvents and associated effects on ICP-OES and ICP-MS stages

Organic solvents can be characterized by specific physico-chemical properties *i.e.* volatility, viscosity, surface tension, density, dissociation energy. They are reported in Table 1 for the most common organic solvents encountered in ICP-related applications. The nature of the solvent will induce variable impacts on the ICP instruments and analytical performances. Depending on the application, different solvents are used. For example, the four most popular organic solvents used in petroleum fields are xylene, kerosene, toluene and hexane [6]. Considering liquid chromatography coupled to ICP, acetonitrile and methanol are the major solvents used in mobile phases. Other solvents such as ethanol, isopropanol, hexane, methylene chloride and tetrahydrofuran can also be encountered [57].

2.1. Definitions and classifications

According to Cohr [58], "the term [organic solvents] is a generic name for a group of organic chemicals or mixtures thereof which typically are liquid in the temperature range of 0-250 °C". These solvents are also relatively chemically inert [58].

Organic solvents, containing at least one carbon atom, can be classified according to various criteria. For example, eight categories can be defined according to their functional groups: hydrocarbons, alcohols, glycol ethers, chlorinated solvents, ketones, ethers, esters and miscellaneous solvents [59]. Many physico-chemical properties can also be used to classify solvents such as melting and boiling points, vapor pressure, heat of vaporization, dissociation energy, volatility, refraction index, density, viscosity, surface tension, dipole moment, relative permittivity, polarizability, specific conductivity, etc. Among all these

properties, surface tension, viscosity, density, volatility and dissociation energy are of major importance regarding the introduction of organic/hydro-organic matrices into ICP sources and plasma stability [10]. However, some properties, such as volatility and dissociation energies, are not tabulated[10]but can be either determined by empirical methods (for example for volatile motor fuels [60]) or approximated from other properties.

Volatility can be considered as an equivalent of the evaporation rate,*i.e.* the amount of evaporated solvent during a given period of time under controlled conditions. This property is linked to other physico-chemical properties such as boiling point, specific heat, vapor pressure, heat of vaporization, etc. Volatility can be approximated using only the boiling point or the specific heat[61]. Dissociation energies are not extensively tabulated either, but can be roughly approximatedby summing the dissociation energy of the chemical bonds of the molecule. Consequently, the higher the number of chemical bonds, the higher the dissociation energy. Thus, dissociation energies for organic solvents are expected to be higher than for water.

Overall, organic solvents exhibit lower surface tension values than water and wide ranges of viscosity, density and volatility[62].From Table 1, it is obvious that pure aqueous and organic/hydro-organic matrices will induce variable effects on the ICP instrumentation, which are discussed in the following sections.

2.2. Impacts of organic/hydro-organic matrices on ICP-OES and ICP-MS stages: from aerosol generation to atomization/excitation/ionization processes

Analyses by ICP techniques involve three main steps before the detection by optical emission or mass spectrometry (Figure 3):

(i) aerosol generation *via* the nebulizer. In this case the liquid sample is transformed into an aerosol consisting of a mixture of droplets and vapor. Generally speaking, the aerosols generated by the nebulizer (*i.e.*, primary aerosols) are too coarse, with around 100 μm maximum drop diameters, to be directly introduced into the plasma. Furthermore, primary aerosols are highly polydispersed in terms of drop diameters and turbulent, with droplets traveling at velocities as high as 80 m s^{-1} . Therefore, an additional step is required.

(ii) aerosol transport through the spray chamber or desolvation system. This step is of crucial importance and its main role is to remove the aerosol coarsest droplets and to reduce the mass of solvent reaching the plasma. Additionally, the turbulences associated to the production of the primary aerosol are reduced and an electrical charge equilibrium is achieved. At the exit of the spray chamber, a finer, less dispersed in terms of drop size diameters and less turbulent aerosol than the primary one is obtained. This is the so-called tertiary aerosol that will be finally introduced into the plasma [63, 64].

(iii) atomization/excitation/ionization in the plasma. Volatilized analytes are converted into free atoms during the atomization, which are then excited (excitation step) and ionized (ionization step) and ions can be further excited.

More details and references on these topics can be found in [6].

To be effectively completed all these processes require adapted introduction systems as well as optimized operating conditions. Details on these two topics are provided in the Part II of this tutorial review. The signal finally obtained depends on the characteristics of the aerosol reaching the plasma both in terms of fineness and mass. The notion of “ideal aerosol” refers to the tertiary aerosol. Ideally, compared to conditions without aerosol, the aerosol reaching the plasma should modify neither excitation temperature and electron number density¹ nor the ions extraction conditions in the case of ICP-MS [67]. Various features have been described to define an ideal aerosol: (i) tertiary aerosol drop size distribution: the drop diameter should be lower than the maximum acceptable by the plasma (*i.e.*, $d \leq 10 \mu\text{m}$); (ii) solvent load: this parameter should span 20 to 40 mg min^{-1} for aqueous matrices, whereas it is solvent dependent in the case of organic/hydro-organic matrices [68]; (iii) dissociation energy: solvents with low dissociation energies will

¹Five fundamental properties of ICP discharges were claimed by Hasegawa and Haraguchi for ICP-OES [65]: plasma temperatures, electron number densities, atom and ion emission lines intensities, number densities of analyte and argon species, and spectral line widths. Two out of the five properties have been particularly studied, namely the plasma excitation temperature and electron number density [65]. Excitation temperature can be defined as the temperature governing the “population density of atomic level p which follows a Boltzmann distribution”. The electron number density is a simpler concept and can be described as “the number of free electrons in a unit volume”. The spatial distribution of excitation temperature and electron number density, in pure aqueous matrices, is well known and has been already discussed in the literature [65, 66].

easily give an “ideal aerosol”; and, (iv) analyte transport rate: this parameter should be maximum [6, 69, 70].

Considering all these features, two are generally reported to characterize the tertiary aerosol: its amount (solvent load and analyte transport) and fineness (drop size distribution), described by various parameters (Table 2) [6]. However, when organic solvents are present, the dissociation energy should also be evaluated for a relevant description of the tertiary aerosol.

The term “solvent load” was introduced by Maessen *et al.* and defined as “the amount (mass) of solvent that enters the plasma in unit time” [68]. The solvent load must be lower than the maximum acceptable so as to minimize the plasma energy consumed by the solvent molecules. Meanwhile, the analyte transport rate must be maximized [6, 69, 70].

The nebulization of organic/hydro-organic matrices generally affects both ICP-OES and ICP-MS at each stage, *i.e.* aerosol generation, aerosol transport, atomization, excitation and ionization steps and for ICP-MS, ion extraction (Figure 3) [10].

Aerosol generation

Usually, a pneumatic nebulizer is employed to produce the primary aerosol. In this case, the solution is exposed to a high velocity gas stream. The gas transfers a fraction of the energy to the liquid stream thus yielding the aerosol. In the case of pneumatically generated aerosols, their properties are mainly affected by the surface tension, the viscosity and the volatility. A surface tension decrease requires less energy to dissociate the liquid and thus induces the production of finer aerosols [71]. A viscosity decrease also leads to the generation of finer aerosols, because it promotes the growing of instabilities on the

liquidsurface during the nebulization event[6, 10]. The volatility acts once the aerosol is produced and may significantly modify its fineness at locations close to the nebulizer tip. As a consequence, finer aerosols are generated in presence of organic/hydro-organic matricesas compared to pure aqueous solutions [10, 72]. Many studies have been conducted to describe the aerosol drop size distribution [73]. Two parameters can help describing the distribution of the primary aerosol: the mean diameter and the span, *i.e.* width of the drop size distribution. Predominantly, empirical expressions have been proposed to model the aerosol mean diameter, among them the $D_{3,2}$, namely the Sauter mean Diameter, has been extensively used.A sample of these models is shown in Table 3. Some models (*e.g.*, Nukiyama-Tanasawa[74, 75]) do not accurately predict the values of $D_{3,2}$, whereas othershave been developed for particular operating conditions (*i.e.*, nebulizer design, liquid and gas flow rates). Nonetheless, all of the shown equations recognize the important role played by the solution surface tension, viscosity and density on the primary aerosol characteristics.

A summary of the impact of each physico-chemical property on the ICP steps is proposed in Table 4. Only few studies have been dedicated in the past to measure the drop size distribution in organic/hydro-organic conditions. However, as seen in Table 4, the main consequence of the presence of organic/hydro-organic matrices is the generation of finer primary aerosolwith respect to pure aqueous media[72, 76, 77]. $D_{3,2}$ was first correlatedwith the surface tension: water and formic acid solutions, with higher surface tension, generated aerosols with higher $D_{3,2}$ than organic solvents (in particular methanol, ethanol, butanol, methyl isobutyl ketone and hexane). Comparing organic solvents with similar surface tension, it was found that the higher the volatility, the lower the $D_{3,2}$ [63]. Besides, organic

solvents lead to a narrower drop size distribution [76, 77]. However, both mean droplet size and span also change with the instrumental and operating conditions [63]. For example, in correlation with the surface tension, two solvent categories were distinguished depending on the shape of the span vs nebulizer gas flow rate: (i) the span reached a maximum and then decreased for organic solvents; while, (ii) it only reached a minimum for water and formic acid solutions. Thus, span slightly varied with the sample uptake rate but significantly with the nebulizer gas flow rate. For $D_{3,2}$, empirical equations have been introduced taking into account the nebulizer gas flow rate [63, 74-76, 78, 79].

Aerosol transport

Normally, the primary aerosol is generated inside a spray chamber, although a desolvation system can be also employed. This aerosol undergoes different processes, called transport phenomena that are responsible for the modification of its fineness and drop number concentration (Figure 4). These events are predominantly solvent evaporation, droplet coalescence and inertial impact losses. In the particular case of organic solvents, the aerosol transport through a spray chamber or a desolvation device, is mainly affected by the solution density and volatility [10]. Higher volatility promotes the solvent evaporation inside the sample introduction devices. This can lead to an increase of the solvent plasma load, S_{tot} [80]. A rise of the solvent volatility also results in an enhancement of the analyte mass reaching the plasma, W_{tot} [6]. A lower density yields coarser tertiary aerosols, higher solvent plasma loads and analyte transport efficiencies [6]. This is due to the fact that an increase in the density gives rise to a growth in the droplets inertia which are therefore more easily removed from the aerosol stream through impacts against the inner chamber walls. As mentioned before, the solvent evaporation plays a very important role in terms of

tertiary aerosol characteristics, analyte and solvent mass delivered to the plasma. Therefore, a deeper consideration of this phenomenon is necessary. Evaporation causes a decrease in the drop diameter (D) at a rate (dD/dt) which is given by[81]:

$$\frac{dD}{dt} = \frac{4D_v M}{R\rho D} \left(\frac{P_\infty}{T_\infty} - \frac{P_d}{T_d} \right) \quad (1)$$

where D_v is the solvent diffusion coefficient, M is its molecular weight, R is the gas constant, ρ is the solvent density, P_∞ and P_d are the partial pressure of the solvent in the carrier gas and the droplet surface, respectively, and T_∞ and T_d are the temperatures in the carrier gas and droplet surface, respectively.

By integrating the previous equation, a relationship between the drop diameter and the time can be found. By considering the change in drop area (dA/dt) caused by evaporation instead of the variation in drop diameter (*i.e.*, $\frac{dA}{dt} = 2\pi D \frac{dD}{dt}$), the previous equation becomes:

$$\frac{dA}{dt} = \frac{8\pi M D_v}{R\rho} \left(\frac{P_\infty}{T_\infty} - \frac{P_d}{T_d} \right) \quad (2)$$

As is may be seen dA/dt is independent of the drop diameter, therefore, the mass of solvent evaporated is proportionally higher for small than for big droplets. This is the so-called Kelvin effect. In fact it has been indicated that only the aerosol finest droplets contribute to the solvent evaporation inside the spray chamber[46]. By considering that some aerosol droplets will not evaporate completely, the Thompson-Gibbs or Kelvin equation should be applied:

$$\frac{P}{P_s} = \exp\left[\frac{4\sigma M}{\rho RTD}\right] \quad (3)$$

where P is the ambient pressure, P_s is the vapour pressure at the temperature T and σ the surface tension.

Therefore, the former equation is transformed into [82]:

$$(D)_t^3 = (D)_0^3 - [48D_v M^2 P_s \sigma (\rho RT)^{-2}]t \quad (4)$$

or:

$$(D)_t^3 = (D)_0^3 - Et \quad (5)$$

where E is the so-called evaporation factor.

The most important assumptions are that the aerosol is under isothermal conditions and that the aerosol flow regime is laminar[83]. The solvent nature plays a very important role from the point of view of aerosol transport, because it affects the evaporation factor. Thus, for instance, this parameter is three times higher for ethanol as compared to water [84].

Analyte atomization/excitation/ionization

The atomization, excitation and ionization processes are influenced by both volatility and dissociation energy [10]. High volatility induces turbulences in the plasma because of the higher amount of solvent mass introduced per time unit. Besides, high dissociation energy involves an increase of the plasma energy required to reach fullmatrix dissociation.

In ICP-MS, these phenomena can induce perturbations during the ion extraction step and generate spectroscopic and/or non-spectroscopic interferences (Chapter 5). In general, efficiency of ion extraction is also affected by the matrix composition [44]. Furthermore, carbon deposition on injector, cones and/or lenses may occur (Section 4.3) [10].

Thus, to summarize, organic/hydro-organic matrices induce antagonistic effects on the aerosol characteristics: beneficial due to the reduction of the mean drop size but detrimental because of the high solvent load and high associated dissociation energy.

2.3. Plasma tolerance and robustness

The organic solvents impact on plasma can be assessed considering plasma tolerance and robustness. Plasma tolerance can be defined as the maximum amount of a substance (solvent load, S_{tot}) that can reach the plasma per time unit without any major instrumental and analytical consequences, such as carbon deposition, plasma extinction, poor stability, low sensitivity. Over time, various criteria and parameters have been considered to describe the notion of tolerance [14, 84-86].

Plasma robustness can be defined as the plasma ability to accept matrix modifications without changes of its fundamental properties, *i.e.* temperature, electron number density, and of the spatial distributions of the species [87].

For both tolerance and robustness, the importance of plasma radio frequency (RF) power and the matching network of the plasma coupling box was particularly stressed.

The following sections review the development of generators and the notions of plasma tolerance and robustness toward organic/hydro-organic matrices in order to point out the

physico-chemical effects behind. Nowadays, the use of lower sample uptake rates makes it easier to increase plasma tolerance and robustness.

Technological developments of RF generators

RF generators and their associating matching boxes are key parts of ICP-OES and ICP-MS spectrometers to obtain both high plasma tolerance and robustness. Over the years, the main modifications of the RF generators have been linked to the need to reduce both their cost and size as well as to improve analytical performances. Various authors have summarized the technical characteristics of commercialized RF generators over time [6, 88-90], Figure 5.

The first studies by ICP-OES were conducted with 5.4 or 7 MHz frequency generators working at 6.6 or 15 kW RF power. More recently, instruments have been equipped with generators working either at 27.12 or 40.68 MHz for ICP-OES or at 27.12, 32 or 40.68 MHz for ICP-MS with RF power in the 1.4-2.0 kW range [6]. Working with a higher frequency (c.a., 40 MHz) offers an improved generator-plasma coupling efficiency which allows improved atomization/excitation/ionization processes and a reduced background continuum intensity in ICP-OES. The former point increases the plasma robustness making it more suitable for the introduction of organic/hydro-organic matrices [6, 91].

The decrease of RF power induces a decrease of electron number density and temperatures in the plasma central channel [92]. As higher solvent load and dissociation energies are involved in presence of organic components, plasma tolerance and robustness towards organic/hydro-organic matrices are expected to be lower than for aqueous matrices.

Notion of tolerance

The notion of tolerance has been investigated through different concepts such as “maximum tolerable aspiration rate”, “limiting aspiration rate”, “ease of introduction”, based on variable instrumental criteria such as evolution of carbon deposition, feasibility of plasma ignition, plasma stability, minimum reflected power values, etc. [14, 68, 84-86]. The experimental studies carried out on a wide range of organic solvents allowed evaluating the degree of plasma tolerance towards these matrices despite the variability of concepts and criteria employed (Table 5). For example, for particularly studied solvents such as nitrobenzene, acetone, hexane, clear common trends can be found.

Several studies have linked the plasma tolerance with physico-chemical properties such as evaporation rate, vapor pressure, etc. [14, 84, 85, 93]. Plasma tolerance towards solvents was shown to be governed firstly by their heat of vaporization, then by parameters impacting the aerosol formation, *i.e.* density, surface tension and viscosity, and also by heat capacity and heat atomization [93]. A rather good correlation was also found between the measured evaporation rates and the “limiting aspiration rates”, *i.e.* plasma showing less tolerance for solvents with high evaporation rates, except for chlorinated hydrocarbons and alcohols [84].

Various empirical relationships between plasma tolerance and physico-chemical properties have also been proposed [84, 93, 94]. Another way to monitor the plasma tolerance is to consider signal intensities dependency with physico-chemical properties (*i.e.* density, viscosity and surface tension) through empirical equations [95, 96].

Plasma tolerance was also linked to solvent chemical structure mainly following: (i) the number of carbon atoms: the higher the number, the lower the plasma tolerance [7]; (ii) the oxygen to carbon ratio: the higher this ratio, the higher the tolerance [85, 97].

In order to help readers to have a rough idea of the plasma tolerance towards a particular solvent, the tolerance (mL min^{-1}) has been plotted as a function of volatility-related properties, *i.e.* evaporation rate, boiling point and specific heat, and also of surface tension, viscosity and density (Figure 6). In this Figure, organic solvents have been classified under three categories according to the plasma tolerance: (i) easy solvents; (ii) intermediate solvents; and, (iii) difficult solvents.

Although no clear trends can be drawn for the so-called "intermediate solvents", an approximate limit value of each property is proposed to classify high and low tolerance solvents: (i) for most solvents with evaporation rates lower than around $100 \mu\text{m}^3 \text{s}^{-1}$, the plasma exhibits a high tolerance; (ii) for boiling points, the limit value shall be set around $100 \text{ }^\circ\text{C}$ with high tolerance above this value; (iii) a surface tension higher than 30 mN m^{-1} generally corresponds to a high tolerance; (iv) for viscosity, the limit shall be fixed at around 1 mPa s with high tolerance above this limit; and, (v) a density higher than 0.85 g mL^{-1} is generally associated with a plasma high tolerance.

The whole considerations discussed above allow to provide indications on plasma tolerance towards organic/hydro-organic matrices. However, experiments have still to be conducted in order to confirm the compatibility of a particular matrix with a given instrumental setup and associated operating parameters.

Notion of robustness

Robustness has been less studied than the tolerance for organic/hydro-organic matrices [98, 99]. As specified above, robustness is characterized by the plasma ability to accept matrix modifications without changes on analyte signals that is to say without changes of plasma fundamental properties *i.e.* temperature, electron number density, and also by keeping a similar spatial distributions of species [87]. A robust plasma is also characterized by the dissociation of the matrix at low plasma height above the load coil (Section 3.2) [100]. Robust conditions are generally achieved at high RF powers, low nebulizer gas flow rates and large inner diameter injectors [6, 87, 101-105], even if, as it will be described in Part II, small inner diameter injectors are often used for organic/hydro-organic matrices analyses.

A common way to assess the matrix dissociation (*i.e.* robustness) by ICP-OES, is to measure ionic (II) -to-atomic (I) line intensities ratio of appropriate elements. Indeed, ionic lines, compared to atomic ones, are more sensitive to plasma conditions modifications. Typically Mg II 280 nm/Mg I 285 nm ratio was considered due to its high sensitivity to plasma conditions modifications and closeness of atomic and ionic lines excitation energies and wavelengths [87, 101, 104].

3. Molecular constituents in the plasma and their spatial distribution

To better understand the impact of organic/hydro-organic matrices on the plasma fundamental properties, a study of the molecular species generated by organic/hydro-organic matrices and their spatial distribution in the plasma with respect to the spatial analytes distribution is of major interest. The pyrolysis products formed in the plasma with pure organic matrices have been addressed by many authors. As seen thereafter, studies were only conducted by ICP-OES.

3.1. Main constituents

For aqueous aerosol, the main molecular constituent in the plasma, OH, is located on the plasma axis between 0 and 10 mm above the load coil (Section 3.2)[106]. In early studies of carbon graphite vapors by mass spectrometry, Drowart *et al.* distinguished five ions: C^+ (11.26 eV), C^{2+} (24.38 eV), C^{3+} (47.89 eV), C^{4+} (64.49 eV) and C^{5+} (392.09 eV). Among them, C^{2+} and C^{3+} were the most abundant [107].

Now considering pure organic matrices and ICP-OES, many species were reported:

- atomic C, C_2 , CH, CN, NH and OH for benzene, carbon tetrachloride and dimethyl sulfoxide, and CS for sulphur-containing solvents[108],
- in decreasing intensities order $CN \geq C_2 \gg CS > OH > NO > CH > NH \geq CCl$ and also atomic C and H in the case of 30 organic solvents[84].

Among these, three main carbon species are considered to be formed in the plasma with nitrogen-containing or nitrogen-free solvents: atomic C, C_2 and CN [84, 109-111]. In the particular case of xylene, mainly atomic C, atomic H and C_2 have been reported [112]. Overall,

organic solvents contribute to the reduction of OH [84], atomic Ar and H [113] band intensities while carbon species intensities increased [84, 113].

Within this frame, two ways were described to monitor the plasma tolerance and robustness during the introduction of organic/hydro-organic matrices using species distribution: *(i)* visual control of the C₂ lines characterized by an intense green visible emission [84] or of the cyanogen bands (CN) with purple color [96, 114]; and, *(ii)* monitoring of band intensities, for example atomic Ar, H and C or C₂ [113].

3.2. Spatial distribution of carbon species

The knowledge of spatial distribution of carbon and non-carbon species is of prime interest [6, 100] in order to: *(i)* better characterize the background that can induce spectral interferences [100]; *(ii)* determine the plasma robustness [100] or tolerance; and, *(iii)* better evaluate the measurement area for an analyte [6].

Considering an axial symmetry of the plasma, spatial distribution of species can be described according to the radial coordinates and the axial coordinates (Figure 7). The latter can be called "observation height", "viewing height", "distance above the load coil" or "height above the load coil" considering ICP-OES and "sampling depth" for ICP-MS [115].

Spatial distribution studies of the main carbon species in the plasma were mainly focused on axial coordinates while only few data are available dealing with radial distributions. Axial distributions are generally similar for atomic C and C₂ according to the literature data, with few contradictions for CN [84, 97, 100, 108, 110-112, 116]. However, their respective band intensities varied depending on the solvents, their concentrations and operating parameters (temperature, RF power, gas flow rates, etc.) [84, 97, 100, 110, 111, 116].

C₂

Overall, C₂ species intensities are centered in the plasma axis and maximum was found around 2 to 10 mm above the load coil [84, 100, 108, 110-112, 116].

Axial distributions were reported depending on the heights above the load coil with: (i) only a maximum at 9 mm above the load coil [108]; (ii) a slow and steady decrease from 5 to 30 mm above the load coil [84]; or, (iii) a quite regular Gaussian-shape, centered between 2 and 7 mm or even higher in the plasma, and intensities still detectable at around 12 mm [100, 110-112, 116].

Considering the radial distribution, C₂ was mainly confined in the central channel of the plasma [97] and around 2-3 mm on each side from the axis [111, 112].

Atomic C

Generally, in ICP-OES, atomic C peaks around 3.5 mm from the plasma center (radial coordinates) and between 5 and 10 mm above the load coil [84, 100, 110, 111], see Figure 8.

For various solvents, considering the axial distribution, atomic C intensities increased drastically from around 2 mm above the load coil to a maximum between 5 and 12 mm (mainly around 5-7 mm), followed by a slow decrease until 30 mm [84, 100, 110, 111].

For the radial distribution measured at 5 mm above the load coil, maximum intensities of atomic C: (i) were steady or increased from the plasma axis to 3.5 mm; (ii) peaked at around 3.5 mm from the plasma axis; and then, (iii) decreased from 3.5 mm to around 7-10 mm from the plasma center [111].

CN

For CN, the spatial distribution varies significantly with the solvent. In general, CN peaks (i) in plasma center around 5 to 10 mm above the load coil and/or(ii) at the edge of the plasmabetween 20 and 30 mm above the load coil [84, 100, 108, 110, 111].

The axial distribution was linked to the chemical composition of the solvents: nitrogen-containing solvents exhibited two peaks, while only one peak, around 15 to 20 mm height above the load coil, was reported for nitrogen-free solvents [84]. However, for this latter kind of solvents, only one peak at 9 mm above the load coil (benzene, carbon tetrachloride and dimethyl sulfoxide) [108], or two peaks (amyl alcohol, carbon tetrachloride, chloroform, toluene, xylene, etc.) [100, 110, 111] were found.

To summarize, Kreuning and Maessen proposed a qualitative picture describing the distribution of the "C₂-tongue", atomic C and CN in the plasma (Figure 8) [111]. According to this figure, C₂ species, located in the plasma center, are firstly dissociated to form atomic C and moved away from the plasma axis. Then, atomic C reacted with nitrogen and/or oxygen coming from the surrounding air to form the CN- and/or CO-species at the outer edges of the plasma [84, 100, 106, 110, 111]. The central CN peak, located at around 5 mm above the load coil, can originate from Ar gas contaminations or analysis of nitrogen-containing solvents [84, 100, 110, 111].

3.3. Spatial distribution of analytes

The spatial distribution of analytes has also been widely studied by ICP-OES. The main trends indicate that the optimum height above the load coil in terms of analytes sensitivities (Cu, P, Mn, Mo, Sr, etc.) is solvent dependent [14, 68, 80, 100, 110, 111, 116-118] (see a selection of studies in Table 6).

Almost all studies were conducted with pure organic matrices[14, 68, 80, 100, 110, 111, 116-118]. Even if the impact of the solvent nature on analyte axial distribution is sometimes difficult to understand[14, 68, 80, 100, 110, 111, 113, 116-119], some studies have shown that analytes and C_2 spatial distributions in the plasma are linked. Some authors have also reported a constant interval in axial coordinates between C_2 and analyte ionic lines maximum emission zone for various solvents and plasma loads [111].

Lower optimum heights above the load coil have been reported for various analytes in pure organic or low organic contents (lower than 2 % v/v) (see Table 6)[14, 80, 113, 117, 118]. This trend was explained by smaller droplets entering the plasma and/or higher desolvation rate due to organic matrices[113]. The situation becomes complex, because in other studies higher optimum heights above the load coil have been obtained for pure organic matrices as compared for water[68, 100, 110, 111, 116]. In this case, an increase in the carbon population, reducing the plasma effective power (see Part II) and delaying the analyte excitation processes has been claimed[110, 116].

Concerning radial distribution, it has been shown that the addition of 2 % (v/v) methanol is able to induce a widening of the analyte distribution which was inversely dependent on the m/z . This modified distribution was correlated with the methanol volatility and background ions C^+ , CO^+ and ArC^+ distribution [120].

4. Impact of organic/hydro-organic matrices on plasma fundamental properties

The carbon species have a direct impact on the plasma fundamental properties, *i.e.* thermal conductivity (transport of dissociation energy) and ionization energy. In order to evaluate this impact, experiments have been conducted to measure the excitation temperature and electron number density with respect to variable organic/hydro-organic matrices. For excitation temperature, authors have used various iron [106, 110, 111, 116, 121, 122], hydrogen [123] or vanadium lines [124] by ICP-OES. In this case, the most commonly employed element is neutral iron, because the atomic lines are located at closely spaced wavelengths over a wide range of energies [125]. The electron number density is generally determined by using hydrogen (H_{β}) line [106, 126]. In this case, the 486.1 nm hydrogen emission line width is significantly affected by the Stark broadening caused by the electric field generated by the plasma electrons and ions [125].

4.1. Excitation temperature

The excitation temperature has been shown to be solvent dependent. Overall, increasing the amount of organic matrices up to a given level induces an increase of the excitation temperature. Above that level the excitation temperature decreases [111, 123, 124]. For example, elevations of the excitation temperature up to 1000 K were reported in ethanol-containing solutions at 15 % [123] and 30 % (v/v) with respect to aqueous media [124], while plasma excitation temperature decreases for higher organic contents. In another study at low RF power values (*e.g.*, 0.75 kW), higher excitation temperatures have been obtained with diluted acetic acid compared to water [122].

However, some studies have reported a systematic 15-25 % excitation temperature decrease in both hydro-organic matrices (20 % (v/v) ethanol) and pure organic (xylene, carbon tetrachloride) [106, 116, 121] whatever the RF power or height above the load coil [106].

To understand the evolution of the excitation temperature in the plasma at various organic contents, temperature spatial distribution studies have been conducted both in radial [106, 121] and axial coordinates (Figure 7) with respect to aqueous conditions [106, 111, 116]. Considering the excitation temperature radial distribution, only a slight distribution broadening and maximum temperature areas modification were noticed at various heights above the load coil [106, 121]. For the axial distribution, maximum excitation temperature was observed at 15 mm above the load coil in aqueous media [106, 116] and shifted at around 20 mm in various organic solvents [106, 111, 116]. In these cases, the maximum excitation temperatures in aqueous media were higher than in organic medium. Due to the dissociation of C_2 species, organic matrices caused a decrease in the available energy on the plasma axis at low heights above the load coil. The maximum excitation temperature is therefore observed at higher heights following the dissociation of all carbon species [106, 111]. This initial excitation temperature decrease can be linked to the different dissociation energies of the main species formed in the plasma: 4.3 eV for OH in aqueous conditions and 6.5 eV for C_2 in organic media. Since the thermal conductivity increases with the dissociation energy of species [127], the thermal conductivity should be higher in organic conditions, leading to a decrease of the excitation temperature in the central channel [106, 128].

In conclusion, it seems that increasing the amount of organic matrices up to a determined level has a positive impact on the plasma excitation temperature. Above that level, increasing further the organic content will lower the plasma excitation temperature.

A way to compensate this effect is to increase the RF power, leading to higher plasma excitation temperature in the central channel associated to an increase of the C/C₂ ratio as shown for example with methyl isobutyl ketone [109, 110, 128]. A RF power increase of about 500 W has also been advocated to optimize ICPs in organic media, leading to similar temperature conditions with respect to aqueous media [106].

4.2. Electron number density

Few studies were conducted to measure the electron number density in organic/hydro-organic matrices. Same trends as those of excitation temperature have been observed with an increase of electron number density from low organic contents up to a determined level followed by a decrease at higher contents [99, 106, 126].

With pure xylene, at 15 mm above the load coil and 2.0 kW power, electron number density was two times lower compared to aqueous media [106]. Electron number density was around 20 % lower with pure ethanol [99] and even lower with ethanol-xylene mixtures [99], with respect to pure aqueous conditions. With pure organic matrices, less energy is available for ionization of the surrounding gas [106], due to the increased solvent load [99].

For hydro-organic samples, up to 25 % ethanol (v/v), the electron number density increased by 1.4-1.7 factor [99, 126]. This rise was, again, followed by a decrease up to 100 % ethanol [99]. Electron number density enhancement was correlated with the increase

of the hydrogen amount, explained by two mechanisms: the lower ionization energy of H compared to Ar, and the production of atomic H from the thermal decomposition of ethanol[126].

In addition, radial distribution of the maximum electron density area was measured at 5, 10 or 15 mm above the load coil[126]. Electron density maximum was observed in the plasma axis with 25 % ethanol whereas it was shifted at 5 mm off axis in aqueous conditions.

4.3. Carbon deposition

Another well-known effect associated to carbon species is the deposition of soot all along the sample path: sample injector, cones and/or lenses due to the incomplete combustion of carbon [6, 10, 43, 44, 53, 129]. In some cases, carbon deposition can induce orifices clogging leading to sensitivity losses, instabilities, interferences and in the extreme case obstruction of the injector or the cones in ICP-MS. The most employed method to reduce carbon deposition is oxygen addition through the use of adapted introduction devices, in the nebulizer, the auxiliary gas flow, etc. For further information on these topics, readers can refer to the Part II of this tutorial review.

5. Spectroscopic and non-spectroscopic interferences

Interferences are commonly divided in two categories:

- spectroscopic or spectral interferences, occurring when atomic or polyatomic ions interfere with the m/z of interesting ICP-MS or when a spectral line interferes with the line of interest using ICP-OES,
- non-spectroscopic or non-spectral interferences, also called matrix effects, observed during the transport and generation of the aerosol or during the atomization, excitation, ionization or ion extraction steps (Figure 3)[43-45].

Both type of interferences need to be eliminated, or at least reduced, for accurate measurements. An overview of spectroscopic and non-spectroscopic interferences associated with organic/hydro-organic matrices is presented hereafter and summarized in Figure 9. Some indications to counteract them are provided while more detailed analytical strategies will be described in the second part of this tutorial review.

5.1. Spectroscopic interferences

Spectroscopic interferences are defined for each type of instrument used (ICP-OES or ICP-MS) and can be very difficult to predict in both cases because they depend on the sample matrix, analytes and analytical conditions. As previously discussed, organic/hydro-organic matrices generate pyrolysis products in the plasma such as atomic C, C₂, CN, CS, CH, CN, etc. which can be considered as the main additional contributors to classical spectroscopic interferences encountered in aqueous conditions.

ICP-OES

Spectral interferences encountered in ICP-OES originate from inherent argon spectrum and additional spectral lines coming from the matrix or the molecular/atomic species. These interferences can be divided in two types: (i) overlap with spectral lines from molecular and atomic species; and, (ii) background continuum variations from matrix.

In order to help analysts to choose the relevant spectral line(s), interferences databases were published (e.g. [130, 131]). For example, the main carbon spectral interferences encountered in ICP-OES are given in Table 7. Preliminary analysis should also help to better anticipate the spectral interferences but in general, solvent-induced spectroscopic interferences are not a limiting factor for trace element analysis in organic/hydro-organic matrices.

ICP-MS

ICP-MS spectroscopic interferences induce intensities increase at the m/z of interest coming from the simultaneous measurement of both the considered isotope and the interfering species, such as M^+ , M^{2+} , MO^+ , MOH^+ , etc. These spectral interferences can be divided into two categories: isobaric interferences, due to overlappings with isotopes of various elements, including doubly charged ions; and polyatomic interferences induced by the presence of atmospheric and plasma gases, solvents, sample matrices, etc. [44, 45].

In order to better anticipate them, extensive compilations of spectroscopic interferences have been published, mainly focused on polyatomic species [132-135]. While isobaric interferences are well known, polyatomic ones are still difficult to predict [136].

Examples of spectroscopic interferences induced by the presence of carbon species in ICP-MS are presented in Table 8, with the indicative required resolving power to overcome them. A convenient way to overcome these induced C spectral interferences can

be the use of double focusing sector field instruments due to their high resolution capabilities [137, 138].

5.2. Non-spectroscopic interferences

Non-spectroscopic interferences have been extensively reviewed (e.g. [43-45, 139]). They are related to the nature and concentration of the matrix, influencing all stages of instrumentation, from the sample introduction to the detection.

High level of organic/hydro-organic matrices generally induce dramatic consequences on instrumentation and analytical performances in ICP techniques.

At low level of organics (from a few percents up to 40 % in some particular cases), a signal enhancement effect can occur. This particular phenomenon has been extensively discussed in the literature either in ICP-OES or ICP-MS. A selection of studies illustrating this effect is presented below.

Signal enhancements in hydro-organic matrices

Experimental studies have been conducted to quantify signal enhancement against various matrices containing methanol [140-143], ethanol [144], acetonitrile [142, 145], methane [146], glycine [147], glycerol [146], glucose [146, 148], amines [149, 150], sodium bicarbonate [151], ammonium carbonate [141], etc. Signal enhancement was shown to increase with carbon content up to a determined value [146], then a more or less drastic decrease of the sensitivity at higher organic contents is observed [142, 146].

In general, signal enhancement can be considered as "element specific" [143, 144] and "carbon source specific". Enhancement varied mainly with the nature and number

offunctional groups of the carbon source, for example –OH, [152]. Signal enhancement were found to be also associated with carbon sources physical states and physico-chemical properties such a boiling point, viscosity, dielectric constant, etc. [152, 153]. To illustrate the effects of variable levels of organic matrices on signal enhancement, a compilation of studies is proposed according to: (1) analytes (Table 9) and (2) carbon sources (Table 10).

In ICP-MS, Allain *et al.* observed signal enhancement for almost all elements with 9-11 eV ionization energies (As, Au, Be, Hg, Se, Te and Zn) which was explained by charge transfer reactions[146]. In another study, signal enhancements were observed for Y (6.22 eV) and Ge (7.90 eV) in diluted acetonitrile solutions and were also linked to charge transfer processes. The authors concluded that the higher the ionization potential, the higher the sensitivity increase and the higher the organic content to reach it [145]. Charge transfer reactions from C⁺ species to analyte atoms (M) may be considered as the main mechanism to explain signal enhancement[147, 154]. It follows the ionization process C⁺-species + M → C-species + M⁺[147]. This mechanism requires a M first ionization energy lower than the positively-charged carbon species ones [155, 156]. C⁺ (11.26 eV) is the main species involved but CO⁺ (14.01 eV), CO₂⁺ (13.77 eV), C₂⁺ (11.4 eV), ArC⁺ and other positively charged molecular carbon species can also play a role [147, 157]. Signal enhancement is also favored for M⁺ with energy close to that of the reactant ion (C⁺) [158, 159]. Besides, conversion of MO⁺ species (MO⁺ + C → M⁺ + CO) can enhance the sensitivity by reducing the refractory oxydes [143, 146]. Considering only this charge transfer mechanism, maximum enhancement factor can be theoretically calculated using the maximum ionization efficiency obtained from the Saha equation [160] (see Table 11). A comparison of experimental enhancement and maximum enhancement factors calculated considering only charge transfer mechanisms (Table 11) showed that for all elements studied with ionization

efficiency lower than 90 %, measured enhancements were higher than the maximum calculated factor, except for B. This phenomenon was also observed, with some exceptions, for analytes with high ionization efficiencies. For example, higher enhancements were reported for Y (6.22 eV), Pb (7.42 eV), Rh (7.46 eV) and Li (5.39 eV)[140, 143] in diluted methanol and acetone, but for Co (7.88 eV), either signal stability [146], or higher enhancements [140] were observed in various hydro-organic matrices. In these studies, a shift of the maximum ion density zone towards the sampler and/or an improved aerosol transport efficiency was suggested in combination with charge transfer mechanisms, to explain the higher enhancements observed[140, 145]. In some cases, electrostatic effects in solution have also been evoked [120].

Signal enhancements depend on the nature of the matrix, its concentration and operating conditions and also on ion mass and ionization energy of the elements in ICP-MS. Various mechanisms have been provided to explain these enhancements in hydro-organic matrices[143, 151, 152, 157, 161-164].

In ICP-OES, the presence of carbon reduces the intensity of some atomic lines for which excitation energies are lower than 6 eV. The signal is enhanced for atomic lines of higher excitation energies, whereas ionic lines are not affected by the presence of carbon[157, 165].

6. Conclusion

The physico-chemical properties of organic/hydro-organic matrices render their introduction into ICP sources particularly challenging due to the associated effects on all stages of instrumentation and analytical performances. This tutorial deals with theoretical considerations of effects induced by such matrices, to better understand the resulting phenomena from the aerosol generation to atomization/excitation/ionization processes.

With respect to aqueous media, these matrices have antagonistic effects on the aerosol characteristics: beneficial due to the reduction of the mean drop size but detrimental because of the high solvent load and high associated dissociation energy. In relation to these aerosol characteristics, plasma tolerance and robustness are affected by the nature of the solvent, its concentration and instrumental setup with associated operating parameters.

The production of carbon molecular constituents is also a consequence of the introduction of organic/hydro-organic matrices in ICP spectrometers, modifying the plasma fundamental properties and species distribution. Up to a given level, carbon content can have beneficial effects on excitation temperature and electron number density. Beyond this level, plasma tolerance and robustness are dramatically affected together with analytical performances. An overview of spectroscopic and non-spectroscopic interferences associated with organic/hydro-organic matrices has also been presented with indications to counteract them.

More detailed practical considerations on instrumentation, such as the choice of adapted introduction devices, as well as instrumental and operating parameters optimization will be presented in Part II, together with analytical strategies for elemental quantification in organic/hydro-organic matrices.

Acknowledgments

We are grateful to the referees, who, through their in depth reviews, have greatly contributed to the improvement of this tutorial review.

References

1. A. Montaser, D.W. Golightly, The Significance of Inductively Coupled Plasmas Relative to Other Laboratory Plasmas in Analytical Spectrometry, in: A. Montaser, D.W. Golightly (Eds.), *Inductively Coupled Plasmas in Analytical Atomic Spectrometry*, VCH Publishers, New York, 1987, pp. 1-15.
2. J. Mora, S. Maestre, V. Hernandis, J.L. Todoli, Liquid-sample introduction in plasma spectrometry, *Trac-Trends in Analytical Chemistry*. 22 (2003) 123-132.
3. A. Montaser, J.A. McLean, H. Liu, An introduction to ICP spectrometries for elemental analysis, in: A. Montaser (Eds.), *Inductively Coupled Plasma Mass Spectrometry*, J. Wiley, Washington, 1998, pp. 1-31.
4. A.A. Ammann, Inductively coupled plasma mass spectrometry (ICP MS): a versatile tool, *Journal of Mass Spectrometry*. 42 (2007) 419-427.
5. D. Profrock, A. Prange, Inductively Coupled Plasma-Mass Spectrometry (ICP-MS) for Quantitative Analysis in Environmental and Life Sciences: A Review of Challenges, Solutions, and Trends, *Applied Spectroscopy*. 66 (2012) 843-868.
6. J.-L. Todoli, J.-M. Mermet, *Liquid Sample Introduction in ICP Spectrometry A Practical Guide*, Elsevier, Oxford, 2008
7. G. Caumette, C.P. Lienemann, I. Merdrignac, H. Paucot, B. Bouyssiere, R. Lobinski, Sensitivity improvement in ICP MS analysis of fuels and light petroleum matrices using

- a microflow nebulizer and heated spray chamber sample introduction, *Talanta*. 80 (2009) 1039-1043.
8. S. Dreyfus, C. Pecheyran, C. Magnier, A. Prinzhofer, C.P. Lienemann, O.F.X. Donard, Direct trace and ultra-trace metals determination in crude oil and fractions by inductively coupled plasma mass spectrometry, *Elemental Analysis of Fuels and Lubricants: Recent Advances and Future Prospects*. 1468 (2005) 51-58.
 9. C.P. Lienemann, S. Dreyfus, C. Pecheyran, O.F.X. Donard, Trace metal analysis in petroleum products: Sample introduction evaluation in ICP-OES and comparison with an ICP-MS approach, *Oil & Gas Science And Technology - Revue D IFP*. 62 (2007) 69-77.
 10. R. Sanchez, J.L. Todoli, C.P. Lienemann, J.M. Mermet, Determination of trace elements in petroleum products by inductively coupled plasma techniques: A critical review, *Spectrochimica Acta Part B-Atomic Spectroscopy*. 88 (2013) 104-126.
 11. A.A. Van Heuzen, ICP-MS in the petroleum industry, in: A.R. Date, A.L. Gray (Eds.), *Applications of Inductively coupled plasma mass spectrometry*, Blackie, Chapman and Hall, New York, 1989, pp. 169-188.
 12. I.B. Brenner, J. Zhu, A. Zander, Evaluation of an ultrasonic nebulizer-membrane separation interface (USN-MEMSEP) with ICP-AES for the determination of trace elements by solvent extraction, *Fresenius Journal of Analytical Chemistry*. 355 (1996) 774-777.
 13. R.M. De Souza, A.L. Saraceno, C. Duyck, C.L.P. da Silveira, R.Q. Aucelio, Determination of Fe, Ni and V in asphaltene by ICPOES after extraction into aqueous solutions using sonication or vortex agitation, *Microchemical Journal*. 87 (2007) 99-103.

14. A. Miyazaki, A. Kimura, K. Bansho, Y. Umezaki, Simultaneous determination of heavy-metals in waters by inductively-coupled plasma atomic emission-spectrometry after extraction into diisobutyl ketone, *Analytica Chimica Acta*. 144 (1982) 213-221.
15. T.B. Wang, X.J. Jia, J. Wu, Direct determination of metals in organics by inductively coupled plasma atomic emission spectrometry in aqueous matrices, *Journal of Pharmaceutical and Biomedical Analysis*. 33 (2003) 639-646.
16. L. Balcaen, G. Woods, M. Resano, F. Vanhaecke, Accurate determination of S in organic matrices using isotope dilution ICP-MS/MS, *Journal Of Analytical Atomic Spectrometry*. 28 (2013) 33-39.
17. J.R. De Souza, C.B. Duyck, T.C.O. Fonseca, T.D. Saint'Pierre, Multielemental determination in oil matrices diluted in xylene by ICP-MS with a dynamic reaction cell employing methane as reaction gas for solving specific interferences, *Journal of Analytical Atomic Spectrometry*. 27 (2012) 1280-1286.
18. S. Jai Kumar, S. Gangadharan, Determination of trace elements in naphtha by inductively coupled plasma mass spectrometry using water-in-oil emulsions, *Journal of Analytical Atomic Spectrometry*. 14 (1999) 967-971.
19. C.M. Andrie, N. Jakubowski, J.A.C. Broekaert, Speciation of chromium using reversed phase-high performance liquid chromatography coupled to different spectrometric detection methods, *Spectrochimica Acta Part B-Atomic Spectroscopy*. 52 (1997) 189-200.
20. U. Arroyo-Abad, S. Lischka, C. Piechotta, J. Mattusch, T. Reemtsma, Determination and identification of hydrophilic and hydrophobic arsenic species in methanol extract of fresh cod liver by RP-HPLC with simultaneous ICP-MS and ESI-Q-TOF-MS detection, *Food chemistry*. 141 (2013) 3093-102.

21. W.Y. Fan, X.J. Mao, M. He, B.B. Chen, B. Hu, Stir bar sorptive extraction combined with high performance liquid chromatography-ultraviolet/inductively coupled plasma mass spectrometry for analysis of thyroxine in urine samples, *Journal of Chromatography A*. 1318 (2013) 49-57.
22. P. Hemstrom, K. Irgum, Hydrophilic interaction chromatography, *Journal of Separation Science*. 29 (2006) 1784-1821.
23. P. Hemstrom, Y. Nygren, E. Bjorn, K. Irgum, Alternative organic solvents for HILIC separation of cisplatin species with on-line ICP-MS detection, *Journal Of Separation Science*. 31 (2008) 599-603.
24. J. Künemeyer, L. Terborg, B.r. Meermann, C. Brauckmann, I. Möller, A. Scheffer, U. Karst, Speciation Analysis of Gadolinium Chelates in Hospital Effluents and Wastewater Treatment Plant Sewage by a Novel HILIC/ICP-MS Method, *Environmental Science & Technology*. 43 (2009) 2884.
25. U. Lindner, J. Lingott, S. Richter, N. Jakubowski, U. Panne, Speciation of gadolinium in surface water samples and plants by hydrophilic interaction chromatography hyphenated with inductively coupled plasma mass spectrometry, *Analytical And Bioanalytical Chemistry*. 405 (2013) 1865-1873.
26. S. Neubauer, A. Rugova, D.B. Chu, H. Drexler, A. Ganner, M. Sauer, D. Mattanovich, S. Hann, G. Koellensperger, Mass spectrometry based analysis of nucleotides, nucleosides, and nucleobases-application to feed supplements, *Analytical and Bioanalytical Chemistry*. 404 (2012) 799-808.
27. Y. Nygren, P. Hemstroem, C. Astot, P. Naredi, E. Bjoern, Hydrophilic interaction liquid chromatography (HILIC) coupled to inductively coupled plasma mass spectrometry (ICPMS) utilizing a mobile phase with a low-volatile organic modifier for the

- determination of cisplatin, and its monohydrolyzed metabolite, *Journal Of Analytical Atomic Spectrometry*. 23 (2008) 948-954.
28. V. Romaris-Hortas, P. Bermejo-Barrera, A. Moreda-Pineiro, Ultrasound-assisted enzymatic hydrolysis for iodinated amino acid extraction from edible seaweed before reversed-phase high performance liquid chromatography-inductively coupled plasma-mass spectrometry, *Journal of Chromatography A*. 1309 (2013) 33-40.
29. C.J. Smith, I.D. Wilson, F. Abou-Shakra, R. Payne, T.C. Parry, P. Sinclair, D.W. Roberts, A comparison of the quantitative methods for the analysis of the platinum-containing anticancer drug {cis-[Amminedichloro(2-methylpyridine)]platinum(II)} (ZD0473) by HPLC coupled to either a triple quadrupole mass spectrometer or an inductively coupled plasma mass spectrometer, *Analytical Chemistry*. 75 (2003) 1463-1469.
30. L. Telgmann, C.A. Wehe, M. Birka, J. Kunemeyer, S. Nowak, M. Sperling, U. Karst, Speciation and Isotope Dilution Analysis of Gadolinium-Based Contrast Agents in Wastewater, *Environmental Science & Technology*. 46 (2012) 11929-11936.
31. D. Xie, J. Mattusch, R. Wennrich, Retention of arsenic species on zwitterionic stationary phase in hydrophilic interaction chromatography, *Journal of Separation Science*. 33 (2010) 817-825.
32. N.H. Bings, J.O.O. von Niessen, J.N. Schaper, Liquid sample introduction in inductively coupled plasma atomic emission and mass spectrometry - Critical review, *Spectrochimica Acta Part B-Atomic Spectroscopy*. 100 (2014) 14-37.
33. A. Montaser, *Inductively Coupled Plasma Mass Spectrometry*, J. Wiley, Washington, 1998
34. A. Montaser, D.W. Golightly, *Inductively Coupled Plasmas in Analytical Atomic Spectrometry*, VCH Publishers, New York, 1987

35. A.W. Moore, Introduction to inductively coupled plasma atomic emission spectrometry. Analytical spectroscopy library, Elsevier, 1989
36. A.R. Date, A.L. Gray, Applications of inductively coupled plasma mass spectrometry, Blackie, Chapman and Hall, New York, 1989
37. P.W.J.M. Boumans, Inductively coupled plasma emission spectroscopy. Part 1, Methodology, instrumentation, and performance, J. Wiley, New York, 1987
38. P.W.J.M. Boumans, Inductively coupled plasma emission spectroscopy. Part 2, Applications and fundamentals, J. Wiley, New York, 1987
39. S.J. Hill, M.J. Bloxham, P.J. Worsfold, Chromatography coupled with inductively-coupled plasma-atomic emission-spectrometry and inductively-coupled plasma-mass spectrometry - A review, *Journal of Analytical Atomic Spectrometry*. 8 (1993) 499-515.
40. M. Montes-Bayon, K. DeNicola, J.A. Caruso, Liquid chromatography-inductively coupled plasma mass spectrometry, *Journal of Chromatography A*. 1000 (2003) 457-476.
41. D. Beauchemin, Inductively coupled plasma mass spectrometry, *Analytical Chemistry*. 78 (2006) 4111-4135.
42. M.J. Cope, G.F. Kirkbright, Some aspects of analytical atomic emission-spectroscopy using inductively coupled plasma sources, *Journal of Physics E-Scientific Instruments*. 16 (1983) 581-590.
43. C. Agatemor, D. Beauchemin, Matrix effects in inductively coupled plasma mass spectrometry: A review, *Analytica Chimica Acta*. 706 (2011) 66.
44. E.H. Evans, J.J. Giglio, Interferences in inductively coupled plasma mass spectrometry. A review, *Journal of Analytical Atomic Spectrometry*. 8 (1993) 1.

45. S.H. Tan, G. Horlick, Matrix-effect observations in inductively coupled plasma mass-spectrometry, *Journal of Analytical Atomic Spectrometry*. 2 (1987) 745-763.
46. B.L. Sharp, Pneumatic nebulizers and spray chambers for inductively coupled plasma spectrometry - A review 2. Spray chambers, *Journal of Analytical Atomic Spectrometry*. 3 (1988) 939-963.
47. B.L. Sharp, Pneumatic nebulizers and spray chambers for inductively coupled plasma spectrometry - A review 1. Nebulizers, *Journal of Analytical Atomic Spectrometry*. 3 (1988) 613-652.
48. J.-L. Todoli, J.-M. Mermet, Sample introduction systems for the analysis of liquid microsamples by ICP-AES and ICP-MS, *Spectrochimica Acta Part B-Atomic Spectroscopy*. 61 (2006) 239-283.
49. V.K. Karandashev, K.V. Zhernokleeva, V.B. Baranovskaya, Y.A. Karpov, Analysis of High-Purity Materials by Inductively Coupled Plasma Mass Spectrometry (Review), *Inorganic Materials*. 49 (2013) 1249-1263.
50. Y. Lecompte, S. Bohand, P. Laroche, A. Cazoulat, Interest and limits of inductively coupled plasma mass spectrometry (ICP-MS) for urinary diagnosis of radionuclide internal contamination, *Annales De Biologie Clinique*. 71 (2013) 269-281.
51. C. Giesen, L. Waentig, U. Panne, N. Jakubowski, History of inductively coupled plasma mass spectrometry-based immunoassays, *Spectrochimica Acta Part B-Atomic Spectroscopy*. 76 (2012) 27-39.
52. D.C. Baxter, I. Rodushkin, E. Engstrom, Isotope abundance ratio measurements by inductively coupled plasma-sector field mass spectrometry, *Journal of Analytical Atomic Spectrometry*. 27 (2012) 1355-1381.

53. K.L. Sutton, J.A. Caruso, Liquid chromatography - inductively coupled plasma mass spectrometry, *Journal of Chromatography A*. 856 (1999) 243.
54. D. Beauchemin, J.C.Y. Leblanc, G.R. Peters, A.T. Persaud, Plasma emission-spectrometry, *Analytical Chemistry*. 66 (1994) R462-R499.
55. A.W. Boorn, R.F. Browner, Chapter 6. Applications: organics, in: P.W.J.M. Boumans (Eds.), *Inductively coupled plasma emission spectroscopy. Part 2, Applications and fundamentals*, J. Wiley, New York, 1987, pp. 151-216.
56. R. Sanchez-Romero, C. Sanchez, C.P. Lienemann, J.-L. Todoli Torro, Metal and metalloid determination in biodiesel and bioethanol, *Journal of Analytical Atomic Spectrometry*. (2014) DOI: 10.1039/C4JA00202D.
57. L.R. Snyder, J.J. Kirkland, J.W. Dolan, *Introduction to Modern Liquid Chromatography*, J. Wiley, Hoboken, 2010
58. K.-H. Cohr (1985) Definition and practical limitation of the concept organic solvents. in *World Health Organization Regional Office for Europe*, pp. 43-55, Copenhagen
59. I.M. Smallwood, *Handbook of organic solvents properties*, New York, 1999
60. ASTM (2009) *Standard Practice for Sampling and Handling of Fuels for Volatility measurement*, D5842-04, West Conshohocken, PA
61. G. Wypych, Solvent volatility, in: G. Wypych (Eds.), *Handbook of Solvents*, ChemTec, Toronto, 2001, pp. 49-50.
62. G. Wypych, Solvent properties, in: G. Wypych (Eds.), *Handbook of Solvents*, ChemTec, Toronto, 2001, pp. 74-75.
63. A. Canals, J. Wagner, R.F. Browner, V. Hernandis, Empirical-model for estimating drop size distributions of aerosols generated by inductively coupled plasma nebulizers, *Spectrochimica Acta Part B-Atomic Spectroscopy*. 43 (1988) 1321-1335.

64. R.F. Browner, A.W. Boorn, D.D. Smith, Aerosol transport model for atomic spectrometry, *Analytical Chemistry*. 54 (1982) 1411-1419.
65. T. Hasegawa, H. Haraguchi, Fundamental Properties of Inductively Coupled Plasmas, in: A. Montaser, D.W. Golightly (Eds.), *Inductively Coupled Plasmas in Analytical Atomic Spectrometry*, VCH Publishers, New York, 1987, pp. 267-322.
66. N.K. Joshi, T.K. Thiagarajan, V.K. Rohatgi, T.S. Ashtamoorthy, The spatial-distribution of excitation temperature and electron-density in an inductively coupled argon plasma, *Journal of Physics D-Applied Physics*. 21 (1988) 1121-1124.
67. A. Montaser, M.G. Minnich, H. Liu, A.G.T. Gustavsson, R.F. Browner, Fundamental aspects of sample introduction in ICP spectrometry, in: A. Montaser (Eds.), *Inductively Coupled Plasma Mass Spectrometry*, J. Wiley, Washington, 1998, pp. 335-420.
68. F. Maessen, G. Kreuning, J. Balke, Experimental Control Of The Solvent Load Of Inductively Coupled Argon Plasmas And Effects Of The Chloroform Plasma Load On Their Analytical Performance, *Spectrochimica Acta Part B-Atomic Spectroscopy*. 41 (1986) 3-25.
69. R.F. Browner, A.W. Boorn, Sample introduction techniques for atomic spectroscopy, *Analytical Chemistry*. 56 (1984) A875-&.
70. R.F. Browner, A. Canals, V. Hernandis, Effect of analyte and solvent transport on signal intensities in inductively coupled plasma atomic emission-spectrometry, *Spectrochimica Acta Part B-Atomic Spectroscopy*. 47 (1992) 659-673.
71. J. Farino, R.F. Browner, Surface-tension effects on aerosol properties in atomic spectrometry, *Analytical Chemistry*. 56 (1984) 2709-2714.

72. J.L. Todoli, A. Canals, V. Hernandis, Behaviour of a single-bore high-pressure pneumatic nebulizer operating with alcohols in inductively coupled plasma atomic emission spectrometry, *Journal of Analytical Atomic Spectrometry*. 11 (1996) 949-956.
73. H.Y. Liu, A. Montaser, Phase-doppler diagnostic studies of primary and tertiary aerosols produced by a high-efficiency nebulizer, *Analytical Chemistry*. 66 (1994) 3233-3242.
74. S. Nukiyama, Y. Tanasawa, An Experiment on the Atomization of Liquid. : 4th Report, The Effect of the Properties of Liquid on the Size of Drops, *Transaction of the Japan Society of Mechanical Engineers*. 5 (1939) 136-143.
75. S. Nukiyama, Y. Tanasawa, Experiments on the Atomization of Liquids in an Air Stream, translated by E. Hope, Defense Research Board, Department of National Defense, Ottawa, Ontario, Canada, 1950
76. K. Kahen, B.W. Acon, A. Montaser, Modified Nukiyama-Tanasawa and Rizk-Lefebvre models to predict droplet size for microconcentric nebulizers with aqueous and organic solvents, *Journal of Analytical Atomic Spectrometry*. 20 (2005) 631-637.
77. S.C.K. Shum, S.K. Johnson, H.M. Pang, R.S. Houk, Spatially resolved measurements of size and velocity distributions of aerosol droplets from a Direct Injection Nebulizer, *Applied Spectroscopy*. 47 (1993) 575-585.
78. N.K. Rizk, A.H. Lefebvre, Spray characteristics of plain-jet airblast atomizers, *Journal of Engineering for Gas Turbines and Power-Transactions of the Asme*. 106 (1984) 634-638.
79. M.S. Elshanawany, A.H. Lefebvre, Airblast atomization - effect of linear scale on mean drop size, *Journal of Energy*. 4 (1980) 184-189.

80. L. Ebdon, E.H. Evans, N.W. Barnett, Simplex optimization fo experimental conditions in inductively coupled plasma atomic emission-spectrometry with organic-solvent introduction, *Journal of Analytical Atomic Spectrometry*. 4 (1989) 505-508.
81. W.C. Hinds, Chapter 13. Condensation and evaporation, in: W.C. Hinds (Eds.), *Aerosol technology*, John Wiley & Sons, New York, 1982, pp. 249-273.
82. M.S. Cresser, R.F. Browner, Observations on the effects of impact beads, mixer paddles, and auxiliary oxident on droplet distributions in analytical flame spectroscopy, *Applied Spectroscopy*. 34 (1980) 364-368.
83. R.F. Browner, Chapter 8. Fundamental aspects of aerosol generation and transport, in: P.W.J.M. Boumans (Eds.), *Inductively coupled plasma emission spectroscopy. Part 2, Applications and fundamentals*, J Wiley, New York, 1987, pp. 244-289.
84. A.W. Boorn, R.F. Browner, Effects Of Organic-Solvents In Inductively Coupled Plasma Atomic Emission-Spectrometry, *Analytical Chemistry*. 54 (1982) 1402-1410.
85. A.W. Boorn, M.S. Cresser, R.F. Browner, Evaporation characteristics of organic-solvent aerosols used in analytical atomic spectrometry, *Spectrochimica Acta Part B-Atomic Spectroscopy*. 35 (1980) 823-832.
86. F. Maessen, P.J.H. Seeverens, G. Kreuning, Analytical aspects of organic-solvent load reduction in normal-power ICPs by aerosol thermostating at low-temperatures, *Spectrochimica Acta Part B-Atomic Spectroscopy*. 39 (1984) 1171-1180.
87. J.M. Mermet, Revisitation of the matrix effects in inductively coupled plasma atomic emission spectrometry: the key role of the spray chamber - Invited lecture, *Journal of Analytical Atomic Spectrometry*. 13 (1998) 419-422.

88. S. Greenfield, Common Radio Frequency Generators, Torches, and Sample Introduction Systems, in: A. Montaser, D.W. Golightly (Eds.), *Inductively Coupled Plasmas in Analytical Atomic Spectrometry*, VCH Publishers, New York, 1987, pp. 1-15.
89. I.L. Turner, A. Montaser, Plasma generation in ICPMS, in: A. Montaser (Eds.), *Inductively Coupled Plasma Mass Spectrometry*, J. Wiley, Washington, 1998, pp. 1-31.
90. C.B. Boss, K.J. Fredeen, *Concepts, instrumentation, and techniques in inductively coupled plasma optical emission spectrometry Second Edition*, Perkin Elmer, USA, 1997
91. M. Huang, S.A. Lehn, E.J. Andrews, G.M. Hieftje, Comparison of electron concentrations, electron temperatures, gas kinetic temperatures, and excitation temperatures in argon ICPs operated at 27 and 40 MHz, *Spectrochimica Acta Part B-Atomic Spectroscopy*. 52 (1997) 1173-1193.
92. B. Capelle, J.M. Mermet, J. Robin, Influence of the generator frequency on the spectral characteristics of inductively coupled plasma, *Applied Spectroscopy*. 36 (1982) 102-106.
93. A.L. Molinero, J.R. Castillo, P. Chamorro, J.M. Muniozguren, Multivariate statistical characterization of the tolerance of argon inductively coupled plasmas to organic solvents, *Spectrochimica Acta Part B-Atomic Spectroscopy*. 52 (1997) 103-112.
94. H. Matsunaga, A new empirical parameter for selection of a suitable solvent used in ICP-AES, *Tohoku Kogyo Gijutsu*. 26 (1993) 25-27.
95. M. Todorovic, S. Vidovic, Z. Ilic, Effect of aqueous-organic solvents on the determination of trace-elements by flame atomic-absorption spectrometry and inductively-coupled plasma-atomic emission-spectrometry, *Journal of Analytical Atomic Spectrometry*. 8 (1993) 1113-1116.

96. S. Greenfield, H.M. McGeachin, P.B. Smith, Nebulization effects with acid solutions in ICP spectrometry, *Analytica Chimica Acta*. 84 (1976) 67-78.
97. D.G. Weir, M.W. Blades, Characteristics of an inductively-coupled argon plasma operating with organic aerosols. 1. Spectral and spatial observations, *Journal of Analytical Atomic Spectrometry*. 9 (1994) 1311-1322.
98. C. Dubuisson, E. Poussel, J.M. Mermet, J.L. Todoli, Comparison of the effect of acetic acid with axially and radially viewed inductively coupled plasma atomic emission spectrometry: influence of the operating conditions, *Journal of Analytical Atomic Spectrometry*. 13 (1998) 63-67.
99. R.I. McCrindle, C.J. Rademeyer, Analytical parameters of ethanol solutions in a 40 MHz inductively coupled plasma optical emission spectrometer, *Journal of Analytical Atomic Spectrometry*. 11 (1996) 437-444.
100. D.G. Weir, M.W. Blades, Characteristics of an inductively-coupled argon plasma operating with organic aerosols. 2. Axial spatial profiles of solvent and analyte species in a chloroform-loaded plasma, *Journal of Analytical Atomic Spectrometry*. 9 (1994) 1323-1334.
101. I. Novotny, J.C. Farinas, J.L. Wan, E. Poussel, J.M. Mermet, Effect of power and carrier gas flow rate on the tolerance to water loading in inductively coupled plasma atomic emission spectrometry, *Spectrochimica Acta Part B-Atomic Spectroscopy*. 51 (1996) 1517-1526.
102. J.W. Tromp, M. Pomares, M. Alvarez-Prieto, A. Cole, H. Ying, E.D. Salin, Exploration of robust operating conditions in inductively coupled plasma mass spectrometry, *Spectrochimica Acta Part B-Atomic Spectroscopy*. 58 (2003) 1927-1944.

103. J.M. Mermet, Ionic to atomic line intensity ratio and residence time in inductively coupled plasma atomic emission-spectrometry, *Spectrochimica Acta Part B-Atomic Spectroscopy*. 44 (1989) 1109-1116.
104. J.M. Mermet, Use of magnesium as a test element for inductively coupled plasma atomic emission-spectrometry diagnostics, *Analytica Chimica Acta*. 250 (1991) 85-94.
105. X. Romero, E. Poussel, J.M. Mermet, The effect of sodium on analyte ionic line intensities in inductively coupled plasma atomic emission spectrometry: Influence of the operating conditions, *Spectrochimica Acta Part B-Atomic Spectroscopy*. 52 (1997) 495-502.
106. M.W. Blades, B.L. Caughlin, Excitation temperature and electron density in the inductively coupled plasma-aqueous vs organic solvent introduction, *Spectrochimica Acta Part B: Atomic Spectroscopy*. 40 (1985) 579.
107. J. Drowart, R.P. Burns, G. Demaria, M.G. Inghram, Mass spectrometric study of carbon vapor, *Journal of Chemical Physics*. 31 (1959) 1131-1132.
108. D.L. Windsor, M.B. Denton, Evaluation of inductively coupled plasma optical emission spectrometry as a method for elemental analysis of organic-compounds, *Applied Spectroscopy*. 32 (1978) 366-371.
109. P. Barrett, E. Pruszkowska, Use Of Organic-Solvents For Inductively Coupled Plasma Analyses, *Analytical Chemistry*. 56 (1984) 1927-1930.
110. C.K. Pan, G.X. Zhu, R.F. Browner, Role of auxiliary gas-flow in organic-sample introduction with inductively coupled plasma atomic emission-spectrometry, *Journal of Analytical Atomic Spectrometry*. 7 (1992) 1231-1237.

111. G. Kreuning, F. Maessen, Effects of the solvent plasma load of various solvents on the excitation conditions in medium power inductively coupled plasmas, *Spectrochimica Acta Part B-Atomic Spectroscopy*. 44 (1989) 367-384.
112. M.W. Blades, P. Hauser, Quantitation Of Sulfur In Xylene With An Inductively-Coupled Plasma Photodiode-Array Spectrometer, *Analytica Chimica Acta*. 157 (1984) 163-169.
113. J.W. Olesik, A.W. Moore, Influence Of Small Amounts Of Organic-Solvents In Aqueous Samples On Argon Inductively Coupled Plasma Spectrometry, *Analytical Chemistry*. 62 (1990) 840-845.
114. A.J. Nobile, R.G. Shuler, J.E.J. Smith, A modified inductively coupled plasma torch for use with methanol solvents, *Atomic Spectroscopy*. 3 (1982) 73-75.
115. P. Verrept, S. Boonen, L. Moens, R. Dams, Solid sampling by electrothermal vaporization-inductively coupled plasma-atomic emission and -mass spectrometry (ETV-ICP-AES/-MS), in: U. Kurfürst (Eds.), *Solid sample analysis - Direct and slurry. Sampling using GF-AAS and ETV-ICP*, Springer, Berlin, 1998, pp. 191-246.
116. C.K. Pan, G.X. Zhu, R.F. Browner, Comparison of desolvation effects with aqueous and organic (carbon-tetrachloride) sample introduction for inductively coupled plasma atomic emission-spectrometry, *Journal of Analytical Atomic Spectrometry*. 5 (1990) 537-542.
117. A. Miyazaki, A. Kimura, Y. Umezaki, Determination of ng mL^{-1} levels of phosphorus in waters by diisobutyl ketone extraction and inductively coupled plasma atomic emission-spectrometry, *Analytica Chimica Acta*. 127 (1981) 93-101.
118. A. Miyazaki, A. Kimura, Y. Umezaki, Indirect determination of sub-ng mL^{-1} levels of phosphorus in waters by di-isobutyl ketone extraction of reduced

- molybdoantimonylphosphoric acid and inductively-coupled plasma emission-spectrometry, *Analytica Chimica Acta*. 138 (1982) 121-127.
119. J. Chirinos, A. Fernandez, J. Franquiz, Multi-element optimization of the operating parameters for inductively coupled plasma atomic emission spectrometry with a charge injection device detector for the analysis of samples dissolved in organic solvents, *Journal of Analytical Atomic Spectrometry*. 13 (1998) 995-1000.
120. S. Liu, D. Beauchemin, Effect of methanol and sodium dodecylsulfate on radial profiles of ion abundance in inductively coupled plasma mass spectrometry, *Spectrochimica Acta Part B-Atomic Spectroscopy*. 61 (2006) 319-325.
121. S. Razic, I.H. Holclajtner-Antunovic, M. Todorovic, The influence of ethanol addition on the spatial emission distribution of traces in a vertical argon stabilized DC arc plasma, *Journal of the Serbian Chemical Society*. 69 (2004) 377-385.
122. T.D. Hettipathirana, A.P. Wade, M.W. Blades, Effects of organic-acids in low-power inductively coupled argon plasma-optical emission-spectroscopy, *Spectrochimica Acta Part B-Atomic Spectroscopy*. 45 (1990) 271-280.
123. R.I. McCrindle, C.J. Rademeyer, Excitation temperature and analytical parameters for an ethanol-loaded inductively-coupled plasma-atomic emission spectrometer, *Journal of Analytical Atomic Spectrometry*. 10 (1995) 399-404.
124. H. Benli, Plasma spectrochemistry in the Peoples-Republic-of-China, *Spectrochimica Acta Part B-Atomic Spectroscopy*. 38 (1983) 81-91.
125. J.M. Mermet, Chapter 10 Spectroscopic diagnostics: basic concepts, in: P.W.J.M. Boumans (Eds.), *Inductively coupled plasma emission spectroscopy*, J. Wiley, New York, 1987, pp. 353-386.

126. R.I. McCrindle, C.J. Rademeyer, Electron-density and hydrogen distribution in an ethanol-loaded inductively-coupled plasma, *Journal of Analytical Atomic Spectrometry*. 9 (1994) 1087-1091.
127. P.W.J.M. Boumans, *Theory of Spectrochemical Excitation*, Hilger & Watts, New York, 1966
128. P.W.J.M. Boumans, M.C. Lux-Steiner, Modification and optimization of a 50 MHz inductively coupled argon plasma with special reference to analyses using organic-solvents, *Spectrochimica Acta Part B-Atomic Spectroscopy*. 37 (1982) 97-126.
129. T. Wang, Liquid Chromatography-Inductively Coupled Plasma Mass Spectrometry (LC-ICP-MS), *Journal of Liquid Chromatography & Related Technologies*. 30 (2007) 807.
130. P.W.J.M. Boumans, *Line Coincidence Tables for Inductively Coupled Plasma Atomic Emission Spectrometry*, Pergamon Press, Oxford, 1980
131. R. Payling, P. Larkins, *Optical Emission Lines of the Elements*, J. Wiley, Chichester, 2000
132. M.A. Vaughan, G. Horlick, Oxide, hydroxide, and doubly charged analyte species in inductively coupled plasma mass-spectrometry, *Applied Spectroscopy*. 40 (1986) 434-445.
133. S.H. Tan, G. Horlick, Background spectral features in inductively coupled plasma mass-spectrometry, *Applied Spectroscopy*. 40 (1986) 445-460.
134. M.A. Vaughan, G. Horlick, A computerized reference manual for spectral data and interferences in ICP-MS, *Applied Spectroscopy*. 41 (1987) 523-526.
135. T.W. May, R.H. Wiedmeyer, A table of polyatomic interferences in ICP-MS, *Atomic Spectroscopy*. 19 (1998) 150-155.

136. H. Vanhoe, J. Goossens, L. Moens, R. Dams, Spectral interferences encountered in the analysis of biological-materials by inductively-coupled plasma-mass spectrometry, *Journal of Analytical Atomic Spectrometry*. 9 (1994) 177-185.
137. P. Pohl, N. Vorapalawut, B. Bouyssiére, H. Carrier, R. Lobinski, Direct multi-element analysis of crude oils and gas condensates by double-focusing sector field inductively coupled plasma mass spectrometry (ICP MS), *Journal of Analytical Atomic Spectrometry*. 25 (2010) 704-709.
138. R.B. Khouzam, R. Lobinski, P. Pohl, Multi-element analysis of bread, cheese, fruit and vegetables by double-focusing sector-field inductively coupled plasma mass spectrometry, *Analytical Methods*. 3 (2011) 2115-2120.
139. J. Marshall, J. Franks, Matrix interferences from methacrylic-acid solutions in inductively coupled plasma mass-spectrometry, *Journal of Analytical Atomic Spectrometry*. 6 (1991) 591-600.
140. E.G. Yanes, N.J. Miller-Ihli, Parallel path nebulizer: Critical parameters for use with microseparation techniques combined with inductively coupled plasma mass spectrometry, *Spectrochimica Acta Part B-Atomic Spectroscopy*. 60 (2005) 555-561.
141. E.H. Larsen, S. Sturup, Carbon-enhanced inductively-coupled plasma-mass spectrometric detection of arsenic and selenium and its application to arsenic speciation, *Journal of Analytical Atomic Spectrometry*. 9 (1994) 1099-1105.
142. C. Demesmay, M. Olle, M. Porthault, Arsenic Speciation By Coupling High-Performance Liquid-Chromatography With Inductively-Coupled Plasma-Mass Spectrometry, *Fresenius Journal Of Analytical Chemistry*. 348 (1994) 205-210.
143. Z.C. Hu, S.H. Hu, S. Gao, Y.S. Liu, S.L. Lin, Volatile organic solvent-induced signal enhancements in inductively coupled plasma-mass spectrometry: a case study of

- methanol and acetone, *Spectrochimica Acta Part B-Atomic Spectroscopy*. 59 (2004) 1463-1470.
144. Z.C. Hu, S. Gao, S.H. Hu, Y.S. Liu, H.H. Chen, A preliminary study of isopropyl alcohol matrix effect and correction in ICP-MS, *Chinese Chemical Letters*. 18 (2007) 1297-1300.
145. A.P. Navaza, J.R. Encinar, M. Carrascal, J. Abián, A. Sanz-Medel, Absolute and Site-Specific Quantification of Protein Phosphorylation Using Integrated Elemental and Molecular Mass Spectrometry: Its Potential To Assess Phosphopeptide Enrichment Procedures, *Analytical Chemistry*. 80 (2008) 1777-1787.
146. P. Allain, L. Jaunault, Y. Mauras, J.M. Mermet, T. Delaporte, Signal Enhancement Of Elements Due To The Presence Of Carbon-Containing Compounds In Inductively Coupled Plasma Mass-Spectrometry, *Analytical Chemistry*. 63 (1991) 1497-1498.
147. A.S. Al-Ammar, E. Reitznerova, R.M. Barnes, Feasibility of using beryllium as internal reference to reduce non-spectroscopic carbon species matrix effect in the inductively coupled plasma-mass spectrometry (ICP-MS) determination of boron in biological samples, *Spectrochimica Acta Part B-Atomic Spectroscopy*. 54 (1999) 1813-1820.
148. J. Machat, V. Kanicky, V. Otruba, Determination of selenium in blood serum by inductively coupled plasma atomic emission spectrometry with pneumatic nebulization, *Analytical and Bioanalytical Chemistry*. 372 (2002) 576-581.
149. C.D. Pereira, E.E. Garcia, F.V. Silva, A.R.A. Nogueira, J.A. Nobrega, Behaviour of arsenic and selenium in an ICP-QMS with collision and reaction interface, *Journal of Analytical Atomic Spectrometry*. 25 (2010) 1763-1768.
150. S.Q. Cao, H.T. Chen, X.J. Zeng, Determination of mercury in biological samples using organic compounds as matrix modifiers by inductively coupled plasma mass spectrometry, *Journal of Analytical Atomic Spectrometry*. 14 (1999) 1183-1186.

151. M. Pettine, B. Casentini, D. Mastroianni, S. Capri, Dissolved inorganic carbon effect in the determination of arsenic and chromium in mineral waters by inductively coupled plasma-mass spectrometry, *Analytica Chimica Acta*. 599 (2007) 191-198.
152. I. Llorente, M. Gomez, C. Camara, Improvement of selenium determination in water by inductively coupled plasma mass spectrometry through use of organic compounds as matrix modifiers, *Spectrochimica Acta Part B-Atomic Spectroscopy*. 52 (1997) 1825-1838.
153. T. Kumamaru, Y. Okamoto, Y. Yamamoto, F. Nakata, Y. Nitta, H. Matsuo, Enhancement effect of organic-solvents in inductively coupled plasma atomic emission-spectrometry, *Fresenius Zeitschrift Fur Analytische Chemie*. 327 (1987) 777-781.
154. F.R. AbouShakra, M.P. Rayman, N.I. Ward, V. Hotton, G. Bastian, Enzymatic digestion for the determination of trace elements in blood serum by inductively coupled plasma mass spectrometry, *Journal of Analytical Atomic Spectrometry*. 12 (1997) 429-433.
155. A.G. Harrison, *Chemical Ionization Mass Spectrometry* 2nd edition, CRC Press, London, 1992
156. R.A. Mapleton, *Theory of charge exchange*, New York, 1972
157. G. Grindlay, J. Mora, M. de Loos-Vollebregt, F. Vanhaecke, A systematic study on the influence of carbon on the behavior of hard-to-ionize elements in inductively coupled plasma-mass spectrometry, *Spectrochimica Acta Part B-Atomic Spectroscopy*. 86 (2013) 42-49.
158. H. Niu, R.S. Houk, Fundamental aspects of ion extraction in inductively coupled plasma mass spectrometry, *Spectrochimica Acta Part B-Atomic Spectroscopy*. 51 (1996) 779-815.

159. J. Machat, V. Otruba, V. Kanicky, Spectral and non-spectral interferences in the determination of selenium by inductively coupled plasma atomic emission spectrometry, *Journal of Analytical Atomic Spectrometry*. 17 (2002) 1096-1102.
160. R.S. Houk, Mass-spectrometry of inductively coupled plasmas, *Analytical Chemistry*. 58 (1986) A97-&.
161. M. Kovacevic, W. Goessler, Direct introduction of volatile carbon compounds into the spray chamber of an inductively coupled plasma mass spectrometer: Sensitivity enhancement for selenium, *Spectrochimica Acta Part B-Atomic Spectroscopy*. 60 (2005) 1357-1362.
162. F. Vanhaecke, R. Dams, C. Vandecastelle, Zone model as an explanation for signal behavior and non-spectral interferences in inductively-coupled plasma-mass spectrometry, *Journal of Analytical Atomic Spectrometry*. 8 (1993) 433-438.
163. F. Vanhaecke, C. Vandecasteele, H. Vanhoe, R. Dams, Study of the intensity of M^+ , M^{2+} and MO^+ signals in ICP-MS as a function of instrumental parameters, *Mikrochimica Acta*. 108 (1992) 41-51.
164. H.P. Longerich, Effect of nitric-acid, acetic-acid and ethanol on inductively coupled plasma mass-spectrometric ion signals as a function of nebulizer gas-flow, with implications on matrix suppression and enhancements, *Journal of Analytical Atomic Spectrometry*. 4 (1989) 665-667.
165. N. Furuta, Spatial emission distribution of YO, Y-I, Y-II and Y-III radiation in an inductively coupled plasma for the elucidation of excitation mechanisms, *Spectrochimica Acta Part B-Atomic Spectroscopy*. 41 (1986) 1115-1129.
166. Web of Science™, apps.webofknowledge.com, Accessed™ 10/16/2014

167. W.M. Haynes, T.J. Bruno, D.R. Lide, CRC Handbook of Chemistry and Physics 94th Edition, <http://www.hbcpnetbase.com/>, 2013
168. F. Albarede, B. Beard, Analytical methods for non-traditional isotopes, in: C.M. Johnson, B.L. Beard, F. Albarede (Eds.), *Geochemistry of Non-Traditional Stable Isotopes*, Mineralogical Soc Amer, Chantilly, 2004, pp. 113-152.
169. A. Zander, The Problem of Spectral Interferences and Line Selection in Plasma Emission Spectrometry, in: A. Montaser, D.W. Golightly (Eds.), *Inductively Coupled Plasmas in Analytical Atomic Spectrometry*, VCH Publishers, New York, 1987, pp. 201-238.
170. Y.-R. Luo, J.-P. Cheng, Bond dissociation energies, in: W.M. Haynes, T.J. Bruno, D.R. Lide (Eds.), *CRC Handbook of Chemistry and Physics 94th Edition*, <http://www.hbcpnetbase.com/>, 2013, pp. 9-65 - 9-96.
171. R.C. Hutton, Application of inductively coupled plasma source-mass spectrometry (ICP-MS) to the determination of trace-metals in organics, *Journal of Analytical Atomic Spectrometry*. 1 (1986) 259-263.

Figures

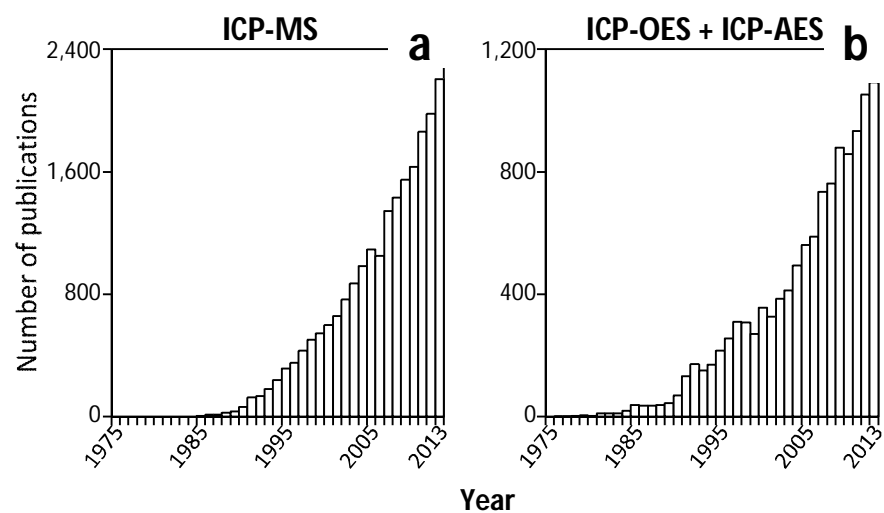


Figure 1: Evolution of publications number associated with a) "ICP-MS" and b) "ICP-AES" and "ICP-OES" topics from 1975 to 2013 (Web of ScienceTM database)[166]

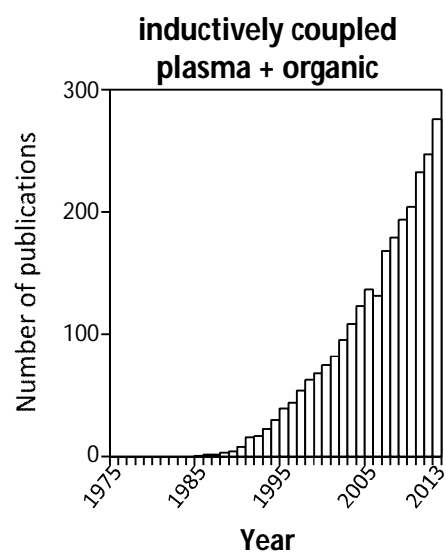


Figure 2: Evolution of the publications number associated with “inductively coupled plasma” and “organic” topics from 1975 to 2013 (Web of Science™ database[166])

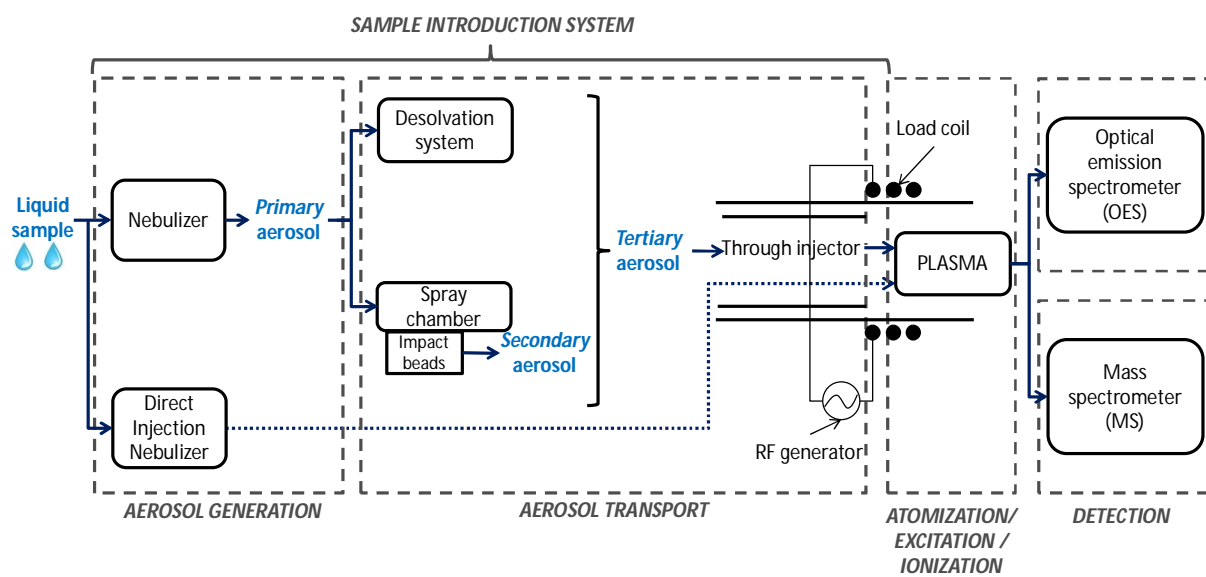


Figure 3: Overview of the ICP-OES and ICP-MS main constituents

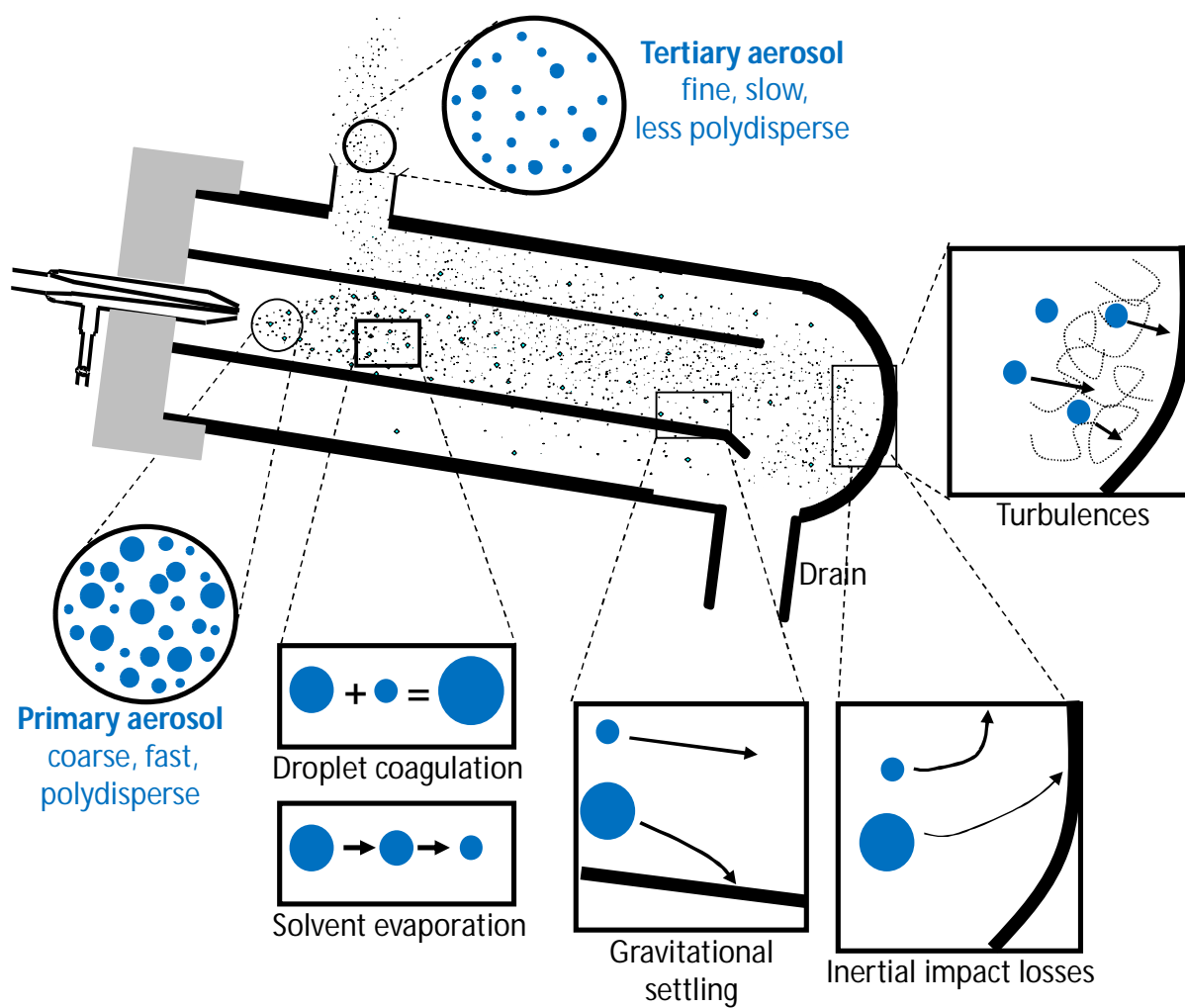


Figure 4: Overview of the aerosol transport processes involved in a concentric nebulizer coupled to a double pass spray chamber (from Todolí and Mermet [6])

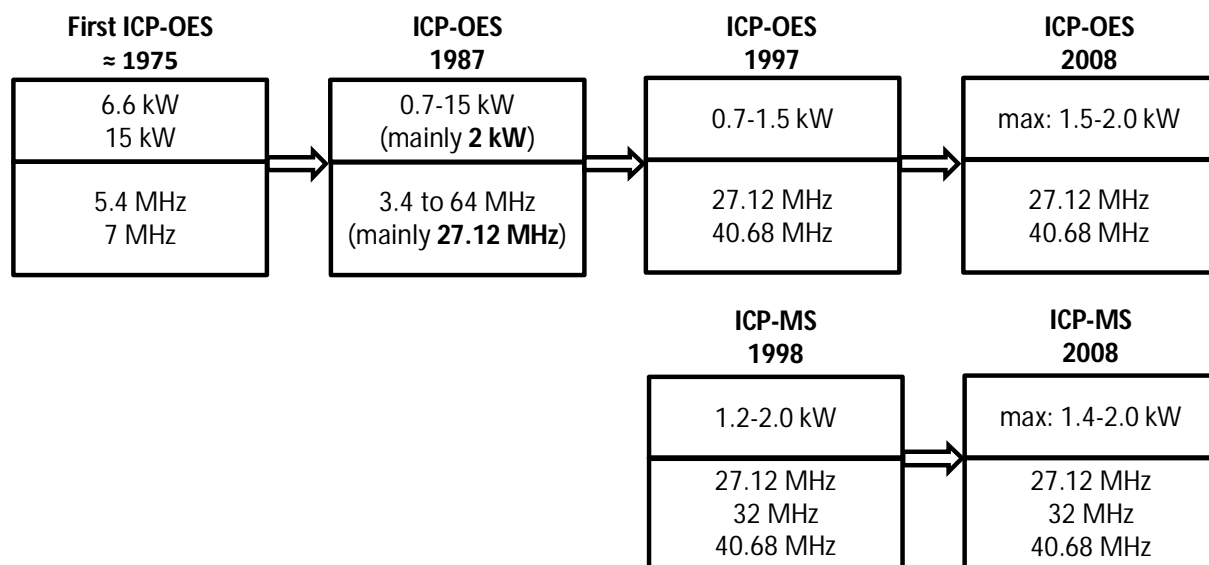


Figure 5: Historical evolution of RF generators for ICP-OES and ICP-MS. The upper boxes contain the RF power and the lower boxes the frequency [6, 88-90].

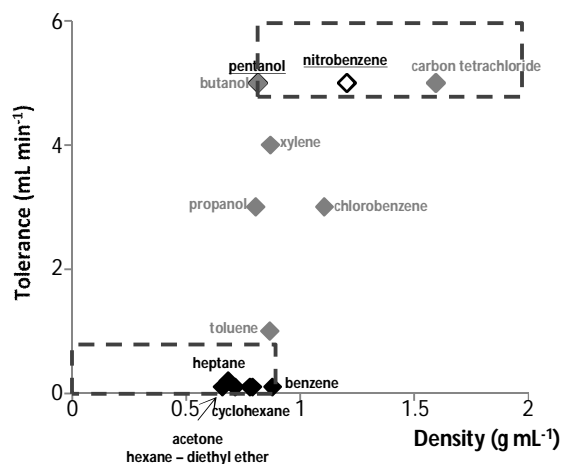
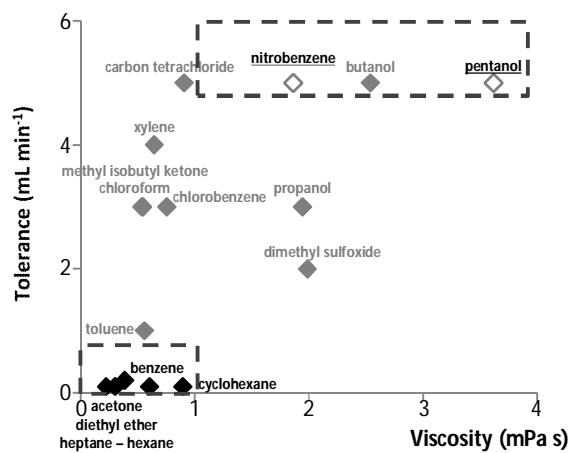
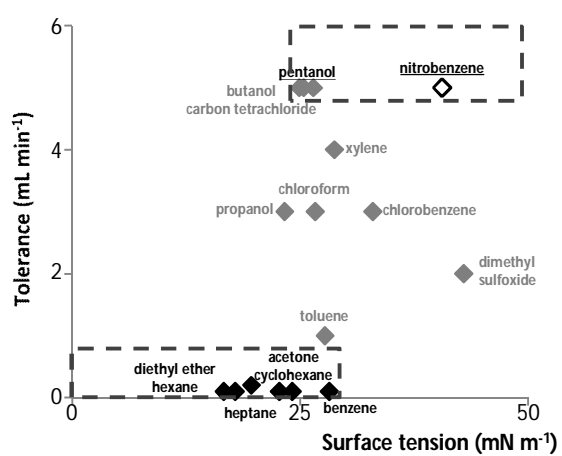
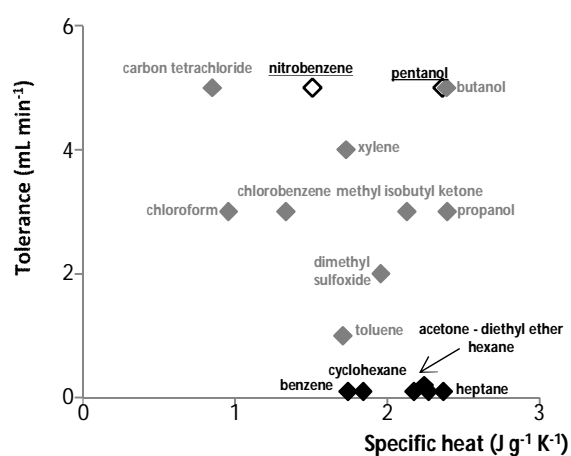
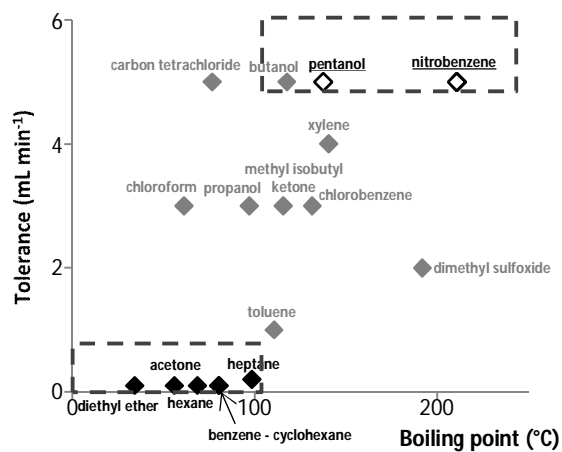
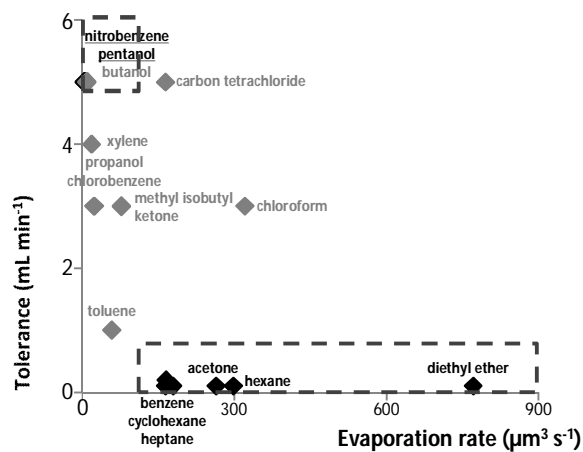
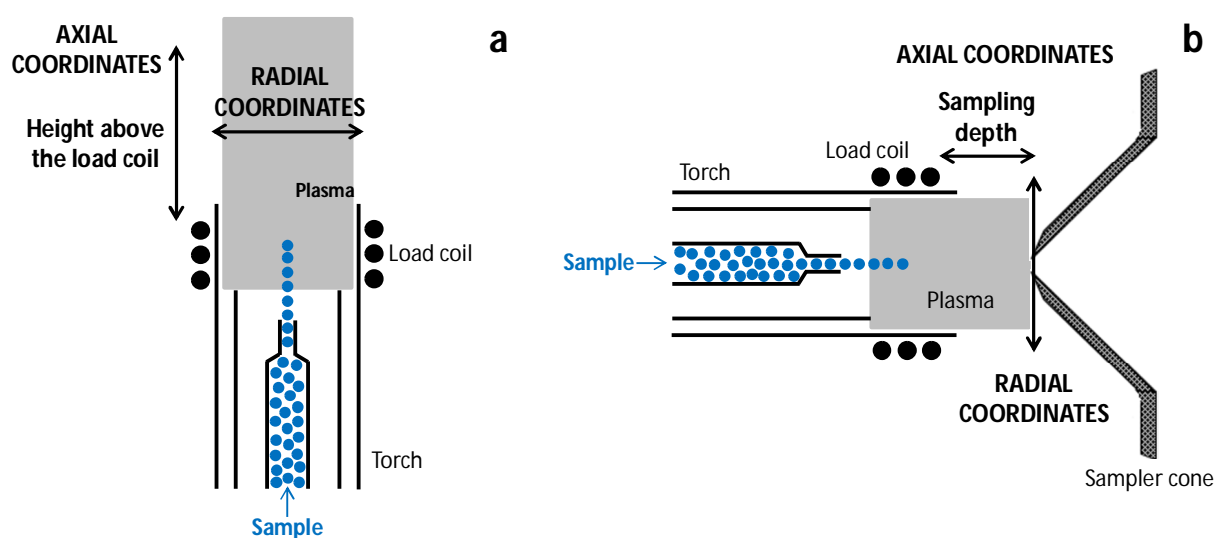


Figure 6: Evolution of the tolerance (in mL min⁻¹) [84] vs evaporation rate (μm³ s⁻¹) [84], boiling point (°C), specific heat (in J g⁻¹ K⁻¹, 25 °C), surface tension (in nN m⁻¹, 25 °C), viscosity (in mPa s, 25 °C) and density (in g mL⁻¹, 20 °C)[167] for various organic solvents classified into three categories according to the plasma tolerance: (i) easy solvents (white diamonds); (ii) intermediate solvents (grey diamonds); and, (iii) difficult solvents (black diamonds) (solvents without referenced physico-chemical data in[167] are not plotted).

Figure 7: Schematic representation of the plasma part of an a) ICP-OES and b) ICP-MS including spatial coordinates (inspired by Albarede and Beard[168] and by Houk[160])



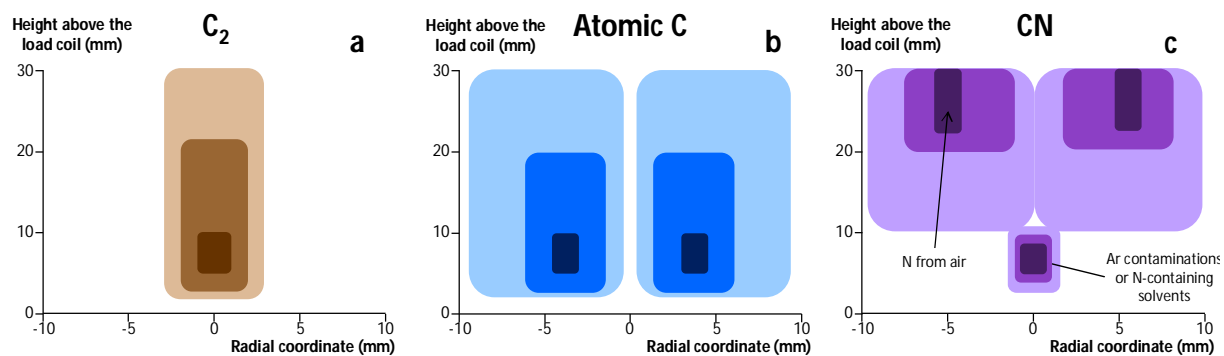


Figure 8: Qualitative pictures of the spatial distribution of a) C_2 , b) atomic C and c) CN in the plasma (dark parts indicate increased intensities) (inspired by Kreuning and Maessen [111])

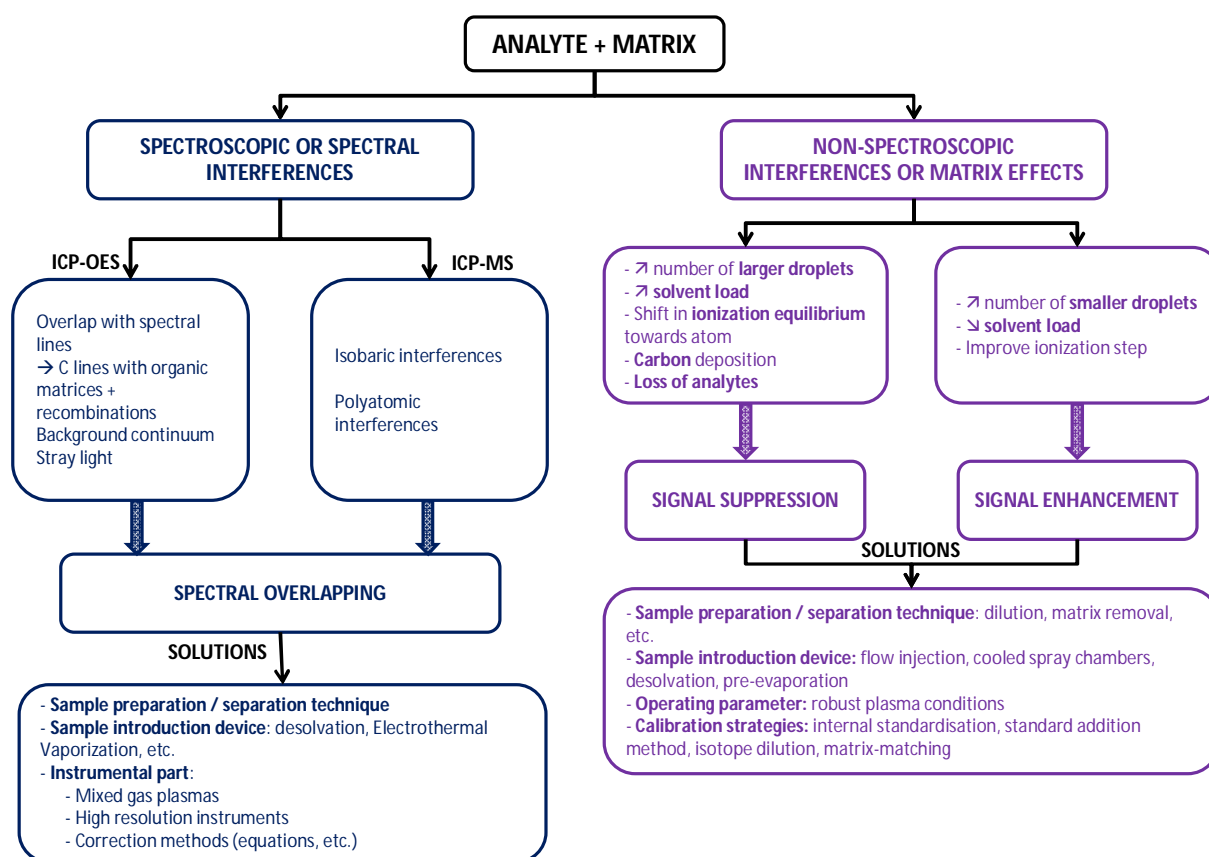


Figure 9: Overview of the spectroscopic and non-spectroscopic interferences and ways to take into account their drawbacks (inspired by Agatemor *et al.*[43]) [44, 169]

Tables

Table 1: Physico-chemical properties of commonly used organic solvents and water in ICP experiments

	Surface tension (mN m ⁻¹) (25 °C)[167]	Viscosity (mPa s) (25 °C)[167]	Density (g mL ⁻¹) (20 °C)[167]	VOLATILITY			Dissociation energy (kJ mol ⁻¹) (25 °C) ¹ [170]
				Boiling point (°C)[167]	Specific heat (J g ⁻¹ K ⁻¹) (25 °C) [167]	Evaporation rate (μm ³ s ⁻¹) [84]	
Water	71.99	0.890	0.99821	100.0	4.180	13.1	860
Methanol	22.07	0.544	0.7909	64.6	2.531	47.2	1992
Ethanol	21.97	1.074	0.7893	78.29	2.438	45.6	3472
Acetonitrile	25.51	0.369	0.7825	81.65	2.229	/	2799
Xylene ²	28.01-29.76	0.581-0.760	0.86-0.88	138.37-144.5	1.710-1.753	18.5	9211
Toluene	27.73	0.560	0.8668	110.63	1.707	58.4	7730
Hexane	17.89	0.300	0.6593	68.73	2.270	298	9134

¹Estimated from the constants of the chemical bonds dissociation energies. ²Extreme values for ortho-, meta- and para-xylene.

Table 2: Selected parameters generally employed to characterize the aerosol entering the plasma [6]

Drop size distribution		Solvent and analyte load	
$D_{3,2}$	Sauter mean diameter - surface mean diameter or ratio of the total volume to the surface area of drops in an aerosol population (μm)	Q_i	Sample uptake rate (mL min^{-1} or $\mu\text{L min}^{-1}$)
$D_{4,3}$	Mass or volume mean diameter (μm)	S_{tot}	Total mass solvent transport rate (mg min^{-1} or $\mu\text{g s}^{-1}$)
D_{50}	Median of the volume drop size distribution (μm)	W_{tot}	Total mass analyte transport rate ($\mu\text{g min}^{-1}$ or $\mu\text{g s}^{-1}$)
		ϵ_n	Analyte transport efficiency
		ϵ_s	Solvent transport efficiency

Table 3: Models employed for the prediction of the Sauter mean diameter of aerosols pneumatically generated.

Model	Comments	Ref.
$D_{3,2} = \frac{585}{V} \sqrt{\frac{\sigma}{\rho}} + 597 \left[\frac{\eta}{\sigma \rho} \right]^{0.45} \left(1000 \frac{Q_l}{Q_g} \right)^{1.5}$	<p>$D_{3,2}$ (μm): surface mean diameter of the drop size distribution of the aerosol, also known as Sauter mean diameter</p> <p>σ (dyn cm^{-1}): solvent surface tension</p>	[74, 75]
<p>Modified Nukiyama-Tanasawa model</p> $D_{3,2} = \frac{86.4}{V} \sqrt{\frac{\sigma}{\rho}} + 105.4 \left[\frac{\eta}{\sigma \rho} \right]^{0.45} \left(\exp \left(-\frac{Q_g}{10^6 Q_l} \right) \right)$	<p>ρ (g cm^{-3}): solution density</p> <p>η (dyn s cm^{-2}): solution viscosity</p> <p>V (m s^{-1}): difference between the velocities of gas and liquid streams at the nebulizer outlet</p> <p>Q_g and Q_l ($\text{cm}^3 \text{s}^{-1}$): volumetric gas and liquid flow rates, respectively</p>	[76]
<p>Rizk and Lefebvre model</p> $D_{3,2} = 0.48 d_l \left(\frac{Q_l}{\rho_g V^2 d_l} \right)^a \left(1 + \frac{Q_l \rho_l}{Q_g \rho_g} \right)^a + 0.15 d_l \left(\frac{\eta_l^2}{\sigma_l \rho_l d_l} \right)^c \left(1 + \frac{Q_l \rho_l}{Q_g \rho_g} \right)$	<p>$D_{3,2}$ (μm): Sauter mean diameter ($a \approx 0.40$; $b \approx 0.40$; $c \approx 0.50$; $f \approx 0.60$; $g \approx 0.10$; $h \approx 0.50$)</p> <p>d_l: liquid outlet diameter</p> <p>d_p: pre-filmer diameter</p> <p>d_h: mean diameter of the gas exit</p>	[78]
<p>Shanawany-Lefebvre model</p> $D_{3,2} = d_h \left(1 + \frac{Q_l \rho_l}{Q_g \rho_g} \right) \left[0.33 \left(\frac{Q_l}{\rho_g V^2 d_p} \right)^f \right] \left(\frac{\rho_l}{\rho_g} \right)^g + 0.68 \left(\frac{\eta_l^2}{\sigma_l \rho_l d_p} \right)^h$	<p>V (m s^{-1}): difference between the gas and liquid velocities at the capillary exits</p> <p>σ (dyne cm^{-1}): solution surface tension ρ (g cm^{-3}): solution density.</p> <p>η: solution viscosity.</p> <p>Q ($\text{cm}^3 \text{s}^{-1}$): volumetric flow rate.</p> <p>In all cases, the subscript 'l' refers to liquid and 'g' to gas.</p>	[79]

Table 4: Effects of physico-chemical properties associated with organic matrices, on the different steps from the aerosol generation to the ion extraction (modified from Sánchez *et al.* [10])

Step	Physical properties	Organic solvents vs water	Consequences
Primary aerosol generation	Surface tension (mN m ⁻¹)	lower	Finer primary aerosol(D _{3,2})
	Viscosity (mPa s)	lower (with exceptions)	
	Volatility	higher (with exceptions)	
Aerosol transport	Volatility	higher (with exceptions)	Higher amount of analyte and solvent in the plasma → higher solvent load (critical) (W _{tot} , S _{tot})
	Density (g mL ⁻¹)	lower	Coarser tertiary aerosol(D _{3,2}) Higher amount of analyte and solvent in the plasma → higher solvent load (critical) (W _{tot} , S _{tot})
Atomization /excitation/ ionization	Volatility	higher (with exceptions)	Plasma turbulence and degradation
	Dissociation energy (kJ mol ⁻¹)	higher	Plasma degradation
Ion	All parameters	/	Carbon depositions, interferences

extraction			
------------	--	--	--

Table 5: Plasma tolerance, expressed as: “maximum tolerable aspiration rate”, defined by no excessive carbon deposition or plasma extinction (in mL min⁻¹)[85]; “limiting aspiration rates”, defined by stable plasma conditions without noticeable carbon deposition during 1 hour (in mL min⁻¹)[84]; “ease of introduction”[14]; “feasibility of the plasma ignition”[86]; and, “maximum tolerable solvent plasma load”, defined by reflected power lower than 75 W and plasma stability at least 8 hours (in mg s⁻¹)[68]. Uptake rates in mL min⁻¹ or mg s⁻¹ are indicated in brackets.

TOLERANCE				
“Maximum tolerable aspiration rate”	Low < 0.5 mL min⁻¹	Intermediate 0.5-6.5 mL min⁻¹	High ≥ 6.5 mL min⁻¹	Ref.
ICP-OES 1.7 kW (1980)	benzene, diethyl ether (< 0.05) hexane (< 0.1) acetone, cyclohexane (0.1) heptane (0.2) toluene (0.4)	methyl isobutyl ketone (1.5) xylene (2.5) chloroform, carbon tetrachloride (3.0)	ethyl acetate (6.5) chlorobenzene, ethanol, methanol, nitrobenzene, butanol, pentanol, propanol (> 6.5)	[85] ¹

"Limiting aspiration rate"	Low < 2 mL min⁻¹	Intermediate 2-5 mL min⁻¹	High ≥ 5 mL min⁻¹	Ref.
ICP-OES 1.75 kW (1982)	benzene, cyclohexane, diethyl ether, hexane, pentane, tetrahydrofuran (< 0.1) acetone, methanol, toluene (0.1) acetonitrile, heptane (0.2) carbon disulfide, isooctane, dimethylformamide (0.5) pyridine (1.0) ethyl acetate (1.5)	decane, dimethyl sulfoxide, dichloromethane (2.0) ethanol, propyl acetate (2.5) chlorobenzene, chloroform, methyl isobutyl ketone, propanol (3.0) xylene (4.0)	butanol, carbon tetrachloride, nitrobenzene, pentanol (> 5.0)	[84] ²

"Ease of introduction"	Impossible	Difficult	Easy	Very easy	Ref.
ICP-OES	acetone,	chloroform,	acetylacetone, amyl	acetic acid,	[14] ³

1.6 kW (1982)	benzene, cyclohexane, ethyl acetate, dioxan, hexane, methanol	ethanol, toluene	acetate, butanol, butyl acetate, isoamyl acetate, isobutyl acetate, isopropanol, methyl isobutyl ketone, propanol	aniline, benzyl alcohol, 2- butoxyethanol, carbon tetrachloride, diisobutyl ketone, diisopropyl ketone, dimethyl sulfoxide, hexanol, nitrobenzene, pyridine, tributyl phosphate, xylene	
-------------------------	--	---------------------	---	--	--

“Feasibility of the plasma ignition”	Not suitable (difficult solvents)	Feasible	Excellent	Ref.
ICP-OES 1.9 kW	ethanol, methanol, isopropanol	chloroform, toluene	butanol, 1,2- dichloroethane,	[86] ³

(1984)			methyl isobutyl ketone, octanol, xylene	
--------	--	--	---	--

"Maximum tolerable solvent plasma load"	Low	Intermediate	High	Ref.
ICP-OES 1.9 kW (1986)	methanol (1.5)		chloroform (> 10.7)	[68] ¹

¹Limits for each group were drawn from the author's conclusions. ²Data are displayed according to the Molinero *et al.* classification[93]. ³No numerical data were given by the authors.

Table 6: ICP-OES studies of height above the load coil (mm) for maximum sensitivity. Lower (bold), higher (italics) or similar (underlined) heights above the load coil for organic vs aqueous matrices. Analyses of aqueous standard solution in pure organic matrices have been preceded by liquid-liquid extraction [14, 117, 118] or dilution in water miscible solvent steps [80, 110, 116].

Solvent / uptake	Analyte	Optimization process	Introduction device / optimum operating parameters ¹	Height above the load coil (mm)			Ref.
PURE ORGANIC MATRICES							
Diisobutyl ketone 1.8 mL min ⁻¹	P	Univariate ²	Concentric nebulizer Neb ³ : 0.7 L min ⁻¹ / 1.6 kW Aux ⁴ : 1.1 L min ⁻¹ / Plasma ⁵ : 13 L min ⁻¹		Water	Diisobutyl ketone	[117]
				PI	16	14	
Diisobutyl ketone 1.8 mL min ⁻¹	Mo, Sb	Univariate	Concentric nebulizer Neb: 0.7 L min ⁻¹ / 1.4-1.5 kW Aux: 1.10-1.25 L min ⁻¹ / Plasma: 14.5-16.0 L min ⁻¹		Water	Diisobutyl ketone	[118]
				Mo II	17	14	
				Sb I	18	14	
Diisobutyl ketone 1.8 mL min ⁻¹	Cd, Cu, Fe, Mo, Ni, Pb, V, Zn	Univariate	Concentric nebulizer Neb: 0.65 L min ⁻¹ / 1.5 kW Aux: 1.2 L min ⁻¹ / Plasma: 13 L min ⁻¹		Water	Diisobutyl ketone	[14]
				Cd⁶	14	14	
				Cu	21	18	
				Fe	17	16	
				Mo	17	14	
				Ni	18	14	
				Pb	18	16	
				V	22	19	
Carbon tetrachloride 0.5 mL min ⁻¹	Ba	Univariate	Concentric nebulizer – glass cylinder spray chamber Neb: 0.9 L min ⁻¹ / 1.5 kW Aux: 1 L min ⁻¹ / Plasma: 14 L min ⁻¹	<i>↗ height above the load coil with carbon tetrachloride vs aqueous matrices (e.g. at 0 °C, 10 mm for water, 16 mm for CCl₄)</i>			[116]
Carbon tetrachloride	Ba	Univariate	Concentric nebulizer – glass cylinder spray chamber	<i>↗ height above the load coil with CCl₄ vs aqueous matrices</i>			[110]

0.5 mL min ⁻¹			Neb: 0.9 L min ⁻¹ / 1.5 kW Aux: 0-2.3 L min ⁻¹ / Plasma: 14 L min ⁻¹					
Chloroform 0.8 mL min ⁻¹	Cr, Cu, Li, Mn	Univariate	Concentric or V-groove nebulizer – spray chamber / T: -52 to 7.5 °C Neb: 0.7 L min ⁻¹ / 1.5-1.9 kW Aux: 1.5 L min ⁻¹ / Plasma: 25 L min ⁻¹	↗ height above the load coil with increasing chloroform load				[68]
Chloroform 1 mL min ⁻¹	Mg	Univariate	Cross-flow nebulizer – double pass spray chamber Neb: 0.65-0.9 L min ⁻¹ / 1.0-1.5 kW Aux: 0.5 L min ⁻¹ / Plasma: 10 L min ⁻¹	↗ height above the load coil with increasing chloroform load				[100]
Toluene 2.0 mL min ⁻¹	Cr, Cu, Fe, Mn, Zn	Univariate	V-groove nebulizer – spray chamber Neb: 0.7 L min ⁻¹ / 1.75 kW Aux: 1.5 L min ⁻¹ / Plasma: 25 L min ⁻¹		Water	Toluene 15 μmol s ⁻¹	Toluene 50 μmol s ⁻¹	[111]
				Cr	≈ 12	≈ 23	≈ 17	
				Cu	≈ 16	≈ 23	≈ 17	
				Fe	≈ 16	≈ 23	≈ 17	
				Mn	≈ 16	≈ 23	≈ 17	
				Zn ¹	≈ 15	≈ 12	≈ 12	
Acetone chloroform cyclohexane methanol Water: 0.65 mL min ⁻¹ Organic: 0.1- 0.7 mL min ⁻¹	Cu Mn	Simplex ⁷ (3 gas flow rates, RF power, temperature, height above the load coil)	V-groove high-solids nebulizer – Scott-type double pass jacketed spray chamber 6 T: -25 to 55 °C Neb: 0.4-3.0 L min ⁻¹ / 1.0-2.5 kW Aux: 0-3.0 L min ⁻¹ / Plasma: 15-34 L min ⁻¹ Height above the load coil: 0-60 mm			Cu	Mn	[80]
				Water		41	18	
				Cyclohexane		32	12	
				Methanol		18	12	
				Hexane ¹		51	20	
				Chloroform		/	16	
				Acetone		32	18	
HYDRO-ORGANIC MATRICES								
Acetone,	Sr	Univariate	Concentric nebulizer – Scott-	↘ height above the load coil with increasing				[113]

acetonitrile, ethanol (0-2 % organic solvent v/v) 1.1 mL min ⁻¹			type double barrel spray chamber Neb: 0.9 L min ⁻¹ / 1.0 kW Aux: 0.9 L min ⁻¹ / Plasma: 10 L min ⁻¹	solvent percentage	
--	--	--	--	--------------------	--

¹Optimum operating parameters in organic conditions. Note that the optimum height above the load coil in aqueous conditions are obtained with specific optimized operated parameters. ²Univariate search: optimization of one parameter, other parameters kept constant. ³Nebulizer gas flow rate. ⁴Auxiliary gas flow rate. ⁵Plasma gas flow rate. ⁶Exception. ⁷Simplex optimization: multivariate optimization based on variable step-size simple algorithm.

Table 7: Compilation of main carbon spectral interferences in ICP-OES. Only carbon lines with sensitivity higher than 100,000 a.u. (arbitrary unit), interfered spectral lines, with wavelengths delta lower than 0.1 nm and sensitivity up to 1 % of those of the carbon lines are considered[131].

Spectral carbon line (nm)	ICP sensitivity (a.u.)	Interfered spectral lines (wavelength delta < 0.1 nm)					
		Spectral line	Sensitivity (a.u.)	Spectral line	Sensitivity (a.u.)	Spectral line	Sensitivity (a.u.)
C I 296.7224	4,300,000	La I	350,000	Hf I	170,000	W I	68,000
		Dy II	260,000	Fe I	140,000	Cr I	62,000
		Cr I	260,000				

C I 296.4839	4,300,000	Gd I	13,000,000	La I	320,000	Re I	87,000
		Hf I	400,000	Nb I	190,000	Ta II	85,000
		Er II	370,000	Nb I	190,000	Zr II	52,000
		La I	330,000	Y I	110,000		

C I 424.6622	1,700,000	Sc II	2,500,000	Nd II	500,000	Nd II	370,000
		U I	1,400,000	Nd II	460,000	Mo I	230,000
		Sm II	640,000	Nd I	410,000	Sm II	150,000
		Gd I	540,000	Nd II	380,000	Tm II	25,000

C II 232.3689	120,000	Yb II	170,000	Co II	10,000	W II	8,400
		Os I	25,000	Ir I	9,400	Nb II	8,000
		Os I	22,000	Nb II	8,600	In I	2,500
		Nb II	17,000				

C II 232.7152	120,000	Pd I	87,000	Ge I	23,000	Ni II	3,300
		Co II	63,000	Fe II	7,100	Bi I	2,900
		Co I	33,000	Nb II	6,800	Fe II	1,400

C II 232.5587	120,000	Ni I	120,000	Co II	14,000	Ta II	5,800
		Co II	63,000	W II	13,000	Ni II	3,300
		Co I	33,000	Pt I	11,000	Fe II	1,400
		Os I	22,000	W II	8,300	Co II	1,300
		Os I	18,000				

C II 232.4857	120,000	Yb II	170,000	Os I	18,000	Ir I	9,400
		Ni I	120,000	Nb II	17,000	Nb II	8,600
		Os I	22,000	W II	13,000	Ta II	5,800
		Os I	22,000	Co II	10,000	In I	2,500

C II 232.8322	120,000	Si II	200,000	Ge I	23,000	Ru II	4,100
		Pd I	87,000	W II	17,000	Bi I	2,900
		W I	68,000	Fe II	7,100		

Table 8: Compilation of carbon related interferences for various isotopes in ICP-MS and associated resolving power to overcome them([133, 135, 136, 171] and references therein)

Isotope	Abundance (%)	Carbon related interferences	Resolving power
^{24}Mg	79.0	$^{12}\text{C}_2^+$	1,600
^{25}Mg	10.0	$^{12}\text{C}_2^1\text{H}^+$, $^{13}\text{C}^{12}\text{C}^+$	1,100 – 1,400
^{26}Mg	11.0	$^{12}\text{C}^{14}\text{N}^+$, $^{12}\text{C}_2^1\text{H}_2^+$, $^{12}\text{C}^{13}\text{C}^1\text{H}^+$	800 – 1,300
^{27}Al	100	$^{12}\text{C}^{15}\text{N}^+$, $^{13}\text{C}^{14}\text{N}^+$, $^1\text{H}^{12}\text{C}^{14}\text{N}^+$	900 – 1,500
^{28}Si	92.2	$^{12}\text{C}^{16}\text{O}^+$	1,600
^{29}Si	4.7	$^{13}\text{C}^{16}\text{O}^+$, $^{12}\text{C}^{17}\text{O}^+$, $^{12}\text{C}^{16}\text{O}^1\text{H}^+$	1,100 – 1,300
^{30}Si	3.1	$^{12}\text{C}^{18}\text{O}^+$, $^{13}\text{C}^{17}\text{O}^+$, $^{13}\text{C}^{16}\text{O}^1\text{H}^+$, $^{12}\text{C}^{17}\text{O}^1\text{H}^+$, $^{12}\text{C}^{16}\text{O}^1\text{H}_2^+$	800 – 1,200
^{31}P	100	$^{13}\text{C}^{18}\text{O}^+$, $^{12}\text{C}^{18}\text{O}^1\text{H}^+$	900 – 1,100
^{44}Ca	2.1	$^{12}\text{C}^{16}\text{O}_2^+$	1,300
^{45}Sc	100	$^{12}\text{C}^{16}\text{O}_2^1\text{H}^+$, $^{13}\text{C}^{16}\text{O}_2^+$	1,100 – 1,200
$^{46}\text{Ti} / ^{46}\text{Ca}$	8.3 / 0.001	$^{13}\text{C}^{16}\text{O}_2^1\text{H}^+$	1,000
^{47}Ti	7.4	$^{12}\text{C}^{35}\text{Cl}^+$	2,700
^{48}Ti	73.7	$^{12}\text{C}_4^+$, $^{36}\text{Ar}^{12}\text{C}^+$	900 – 2,400
^{49}Ti	5.4	$^{36}\text{Ar}^{13}\text{C}^+$, $^{36}\text{Ar}^{12}\text{C}^1\text{H}^+$, $^{12}\text{C}^{37}\text{Cl}^+$	1,800 – 2,700
^{51}V	99.8	$^{38}\text{Ar}^{13}\text{C}^+$	2,300
^{52}Cr	83.8	$^{40}\text{Ar}^{12}\text{C}^+$	2,400
^{53}Cr	9.5	$^{40}\text{Ar}^{13}\text{C}^+$	2,100
^{60}Ni	26.2	$^{12}\text{C}^{16}\text{O}_3^+$	1,100

^{63}Cu	69.2	$^{36}\text{Ar}^{12}\text{C}^{14}\text{N}^1\text{H}^+$, $^{14}\text{N}^{12}\text{C}^{37}\text{Cl}^+$, $^{16}\text{O}^{12}\text{C}^{35}\text{Cl}^+$	1,300 – 1,800
^{65}Cu	30.9	$^{12}\text{C}^{16}\text{O}^{37}\text{Cl}^+$, $^{12}\text{C}^{18}\text{O}^{35}\text{Cl}^+$	1,600 – 2,000
^{75}As	100	$^{23}\text{Na}^{12}\text{C}^{40}\text{Ar}$, $^{12}\text{C}^{31}\text{P}^{16}\text{O}_2^+$	1,800 – 2,500
^{77}Se	7.6	$^{12}\text{C}^{19}\text{F}^{14}\text{N}^{16}\text{O}_2^+$	1,100

Table 9: Compilation of selected examples resulting in signal enhancement higher than 1.1 for analytes classified according to their ionization energies. Main enhancement mechanisms are indicated

Analyte (ionization energy)	Carbon source (C)	C (g L ⁻¹)	Signal enhancement		Instrumentation (sample uptake, RF power, Neb, height above the load coil or sampling depth)	Ref.
			Factor	Principal source		
Rb (4.18 eV)	Acetone(≈ 0.6 %)	≈ 3	≈ 1.2	Aerosol ¹	ICP-MS, 0.33 mL min ⁻¹ , 1.3 kW, 1.05 L min ⁻¹	[161]
	Methanol (≈ 5 %)	≈ 15	≈ 1.2	Aerosol		
In (5.79 eV)	Isopropanol (≈ 0.08 mol L ⁻¹ / ≈ 0.8 %)	≈ 2.9	≈ 1.8	Aerosol	ICP-MS, 1 mL min ⁻¹ , 1.15 kW, 0.85 L min ⁻¹ , 8 mm	[144]
Al (5.99 eV)	Sodium dodecylsulfate (SDS) (0.2 % m/v)	≈ 1.0	≈ 2	Aerosol + electrostatic effects	ICP-MS, 0.65 mL min ⁻¹ , 1.35 kW, 0.87 L min ⁻¹	[120]
Y (6.22 eV)	Acetonitrile (20 %)	≈ 90	≈ 1.6	Charge transfer ²	ICP-MS ³	[145]
	Methanol (20 %)	≈ 59	5	Aerosol + (charge transfer) ⁴	ICP-MS, 340 nL min ⁻¹ + 15 μL min ⁻¹ make-up flow, 1 kW, 1 L min ⁻¹	[140]
Pb (7.42 eV)	Methanol (2 %)	≈ 6	≈ 1.4	Aerosol + electrostatic effects	ICP-MS, 0.65 mL min ⁻¹ , 1.5 kW, 0.87 L min ⁻¹	[120]
	Methanol (20 %)	≈ 59	6	Aerosol + (charge transfer)	ICP-MS, 340 nL min ⁻¹ + 15 μL min ⁻¹ make-up flow, 1 kW, 1 L min ⁻¹	[140]
Rh (7.46 eV)	Methanol (20 %)	≈ 59	12	Aerosol + (charge transfer)	ICP-MS, 340 nL min ⁻¹ + 15 μL min ⁻¹ make-up flow, 1 kW, 1 L min ⁻¹	[140]
Ni (7.64 eV)	Sodium dodecylsulfate (SDS) (0.2 % m/v)	≈ 1.0	≈ 1.4	Aerosol + electrostatic effects	ICP-MS, 0.65 mL min ⁻¹ , 1.35 kW, 0.87 L min ⁻¹	[120]
Mg (7.65 eV)	Methanol (20 %)	≈ 59	31	Aerosol + possible charge transfer	ICP-MS, 340 nL min ⁻¹ + 15 μL min ⁻¹ make-up flow, 1 kW, 1 L min ⁻¹	[140]

Cu (7.73 eV)	Isopropanol ($\approx 0.08 \text{ mol L}^{-1}$ / $\approx 0.8 \%$)	≈ 2.9	≈ 1.5	Aerosol	ICP-MS, 1 mL min^{-1} , 1.15 kW , 0.85 L min^{-1} , 8 mm	[144]
	Sodium dodecylsulfate (SDS) (0.2% m/v)	≈ 1.0	≈ 1.2	Aerosol + electrostatic effects	ICP-MS, 0.65 mL min^{-1} , 1.35 kW , 0.87 L min^{-1}	[120]
Co (7.88 eV)	Methanol (20 %)	≈ 59	17	Aerosol + possible charge transfer	ICP-MS, 340 mL min^{-1} + $15 \mu\text{L min}^{-1}$ make-up flow, 1 kW , 1 L min^{-1}	[140]
	Sodium dodecylsulfate (SDS) (0.2% m/v)	≈ 1.0	≈ 1.5	Aerosol + electrostatic effects	ICP-MS, 0.65 mL min^{-1} , 1.35 kW , 0.87 L min^{-1}	[120]
Ge (7.90 eV)	Acetonitrile (30 %)	≈ 140	≈ 2.4	Possible charge transfer	ICP-MS ³	[145]
B (8.30 eV)	Glycine ($\approx 6 \%$ (m/v))	20	1.5	Charge transfer + carbon space charge effect + (other species space charge effects)	ICP-MS, 1 mL min^{-1} , 1 kW , 1.0 L min^{-1}	[147]
Sb (8.61 eV)	Methanol (2 %)	≈ 6	≈ 1.4	Aerosol + electrostatic effects + charge transfer	ICP-MS, 0.65 mL min^{-1} , 1.5 kW , 0.87 L min^{-1}	[120]
	Methanol (3 %)	≈ 9	1.5	Aerosol + charge transfer	ICP-MS, 1 mL min^{-1} , 1.32 kW , 0.949 L min^{-1}	[141]
	Sodium dodecylsulfate (SDS) (0.2% m/v)	≈ 1.0	≈ 1.2	Aerosol + electrostatic effects + charge transfer	ICP-MS, 0.65 mL min^{-1} , 1.35 kW , 0.87 L min^{-1}	[120]
Cd (8.99 eV)	Acetone ($\approx 0.6 \%$)	≈ 3	≈ 1.3	Aerosol	ICP-MS, 0.33 mL min^{-1} , 1.3 kW , 1.05 L min^{-1}	[161]
	Methanol ($\approx 5 \%$)	≈ 15	≈ 1.4			
Te (9.01 eV)	Glycerol (1 mol L^{-1})	≈ 36	1.9	Ionization equilibrium modification due to C species	ICP-OES, 1 mL min^{-1} , 1.2 kW , 0.85 L min^{-1}	[146]
	Methane (4%) ⁵	≈ 20	≈ 3.5			
Au (9.23 eV)	Glycerol (1 mol L^{-1} / $\approx 7 \%$)	≈ 36	3.25			

Be (9.32 eV)	Glycine ($\approx 6\%$ m/v)	20	1.15	Charge transfer + carbon space charge effect + (other species space charge effects)	ICP-MS, 1 mL min^{-1} , 1 kW, 1.0 L min^{-1}	[147]
	Isopropanol ($\approx 0.08\text{ mol L}^{-1}$ / $\approx 0.8\%$)	≈ 2.9	≈ 1.5	Aerosol + (charge transfer)	ICP-MS, 1 mL min^{-1} , 1.15 kW, 0.85 L min^{-1} , 8 mm	[144]
Zn (9.39 eV)	Isopropanol ($\approx 0.08\text{ mol L}^{-1}$ / $\approx 0.8\%$)	≈ 2.9	≈ 1.8	Aerosol + possible charge transfer	ICP-MS, 1 mL min^{-1} , 1.15 kW, 0.85 L min^{-1} , 8 mm	[144]
	Sodium dodecylsulfate (SDS) (0.2% m/v)	≈ 1.0	≈ 1.4	Aerosol + electrostatic effects + charge transfer	ICP-MS, 0.65 mL min^{-1} , 1.35 kW, 0.87 L min^{-1}	[120]
Se (9.75 eV)	Acetic acid ($\approx 40\%$)	≈ 170	≈ 3.0	Charge transfer + possible aerosol	ICP-MS, 0.33 mL min^{-1} , 1.3 kW, 1.05 L min^{-1}	[161]
	Acetone ($\approx 2\%$)	≈ 10	≈ 4.4	Aerosol + charge transfer		
	Acetonitrile (30%)	≈ 140	≈ 7.3	Charge transfer	ICP-MS ³	[145]
	Blood serum	/	3	Charge transfer	ICP-MS, 1.35 mL min^{-1} , 1.4 kW, 0.914 L min^{-1}	[154]
	Butanol (1%)	≈ 5	≈ 2.5	Aerosol + charge transfer	ICP-MS, 1 mL min^{-1} , 1.15 kW, neb : variable	[152]
	CFA-C (amine) (10%)	/	1.5 (⁷⁷ Se), 1.3 (⁸² Se)	/ ^b	ICP-MS, 1 mL min^{-1} , 1.4 kW, 0.9 L min^{-1}	[149]
	Ethanol (2%)	≈ 8	≈ 3.5	Aerosol + charge transfer	ICP-MS, 1 mL min^{-1} , 1.15 kW, neb : variable	[152]
	Glucose ($\approx 0.15\text{ mol L}^{-1}$)	10	1.4	Charge transfer	ICP-OES, 1 mL min^{-1} , 1 kW, 0.75 L min^{-1} , 15 mm	[148]
Glycerol (1 mol L^{-1} / $\approx 7\%$)	≈ 36	2.5	Ionization equilibrium modification due to C species	ICP-OES, 1 mL min^{-1} , 1.2 kW, 0.85 L min^{-1}	[146]	

	Isopropanol ($\approx 0.1 \text{ mol L}^{-1} / \approx 1 \%$)	≈ 3.6	≈ 2.5	Aerosol + charge transfer	ICP-MS, 1 mL min^{-1} , 1.15 kW , 0.85 L min^{-1} , 8 mm	[144]
	Methane (4 %)	≈ 20	≈ 3.5	Ionization equilibrium modification due to C species	ICP-OES, 1 mL min^{-1} , 1.2 kW , 0.85 L min^{-1}	[146]
	Methanol (2 %)	≈ 5.9	≈ 3	Aerosol + charge transfer	ICP-MS, 1 mL min^{-1} , 1.15 kW , neb : variable	[152]
	Methanol (3 %)	≈ 9	3.4 (Se^{VI}), 3.1 (SeMet)	Aerosol + charge transfer	ICP-MS, 1 mL min^{-1} , 1.32 kW , 0.949 L min^{-1}	[141]
	Methanol ($\approx 10 \%$)	≈ 30	≈ 3.1	Aerosol + charge transfer	ICP-MS, 0.33 mL min^{-1} , 1.3 kW , 1.05 L min^{-1}	[161]
	Methanol (20 %)	≈ 59	6	Charge transfer + aerosol	ICP-MS, $340 \text{ mL min}^{-1} + 15 \mu\text{L min}^{-1}$ make-up flow, 1 kW , 1 L min^{-1}	[140]
	Propanol (1 %)	≈ 5	≈ 2	Aerosol + charge transfer	ICP-MS, 1 mL min^{-1} , 1.15 kW , neb : variable	[152]
	Sodium bicarbonate (25 mmol L^{-1})	≈ 0.3	1.5	Charge transfer	ICP-MS, 1.5 kW , 1.1 L min^{-1} , 7 mm	[151]
	Sodium dodecylsulfate (SDS) (0.2% m/v)	≈ 1.0	≈ 1.2	Aerosol + electrostatic effects + charge transfer	ICP-MS, 0.65 mL min^{-1} , 1.35 kW , 0.87 L min^{-1}	[120]
As (9.79 eV)	Acetic acid ($\approx 40 \%$)	≈ 170	≈ 3.1	Charge transfer + possible aerosol	ICP-MS, 0.33 mL min^{-1} , 1.3 kW , 1.05 L min^{-1}	[161]
	Acetone ($\approx 2 \%$)	≈ 10	≈ 4.4	Aerosol + charge transfer		
	Acetonitrile (2 %)	≈ 9	≈ 2.8	Ionization equilibrium modification due to C species	ICP-MS, 0.4 mL min^{-1} , 1.4 kW , 0.8 L min^{-1}	[142]
	Acetonitrile (30 %)	≈ 140	≈ 6.1	Charge transfer	ICP-MS ³	[145]
	Ammonium carbonate ($\approx 0.3 \text{ mol L}^{-1}$)	4	2.3 (As^{III})	Charge transfer	ICP-MS, 1 mL min^{-1} , 1.32 kW , 0.949 L min^{-1}	[141]
	CFA-C (amine) (10 %)	/	2.1	/	ICP-MS, 1 mL min^{-1} , 1.4 kW , 0.9 L min^{-1}	[149]

	Glycerol (1 mol L ⁻¹ / ≈ 7 %)	≈ 36	2.4	Ionization equilibrium modification due to C species	ICP-OES, 1 mL min ⁻¹ , 1.2 kW, 0.85 L min ⁻¹	[146]
	Methane (4 %)	≈ 20	≈ 5.5			
	Methanol (2 %)	≈ 5.9	≈ 2	Aerosol + electrostatic effects + charge transfer	ICP-MS, 0.65 mL min ⁻¹ , 1.5 kW, 0.87 L min ⁻¹	[120]
	Methanol (3 %)	≈ 9	3.4(As ^{III}), 4.2 (DMA), 4.5 (AsB)	Aerosol + charge transfer	ICP-MS, 1 mL min ⁻¹ , 1.32 kW, 0.949 L min ⁻¹	[141]
	Methanol (5 %)	≈ 15	≈ 2.3	Ionization equilibrium modification due to C species	ICP-MS, 0.4 mL min ⁻¹ , 1.4 kW, 0.8 L min ⁻¹	[142]
	Methanol (≈ 10 %)	≈ 30	≈ 3.5	Aerosol + charge transfer	ICP-MS, 0.33 mL min ⁻¹ , 1.3 kW, 1.05 L min ⁻¹	[161]
	Methanol (20 %)	≈ 59	31	Charge transfer + aerosol	ICP-MS, 340 mL min ⁻¹ + 15 μL min ⁻¹ make-up flow, 1 kW, 1 L min ⁻¹	[140]
	Sodium bicarbonate (25 mmol L ⁻¹)	≈ 0.3	1.5	Charge transfer	ICP-MS, 1.5 kW, 1.1 L min ⁻¹ , 7 mm	[151]
	Sodium dodecylsulfate (SDS) (0.2 % m/v)	≈ 1.0	≈ 1.5	Aerosol + electrostatic effects + charge transfer	ICP-MS, 0.65 mL min ⁻¹ , 1.35 kW, 0.87 L min ⁻¹	[120]
Hg (10.44 eV)	Acetic acid (≈ 40 %)	≈ 170	≈ 1.7	Possible aerosol	ICP-MS, 0.33 mL min ⁻¹ , 1.3 kW, 1.05 L min ⁻¹	[161]
	Acetone (≈ 2 %)	≈ 10	≈ 1.8	Aerosol		
	Ethylenediamine (6 %)	≈ 22	1.5	Aerosol	ICP-MS, 1 mL min ⁻¹ , 1.35 kW, 0.60 L min ⁻¹ , 8 mm	[150]
	Glycerol (1 mol L ⁻¹ / ≈ 7 %)	≈ 36	6	Ionization equilibrium modification due to C species	ICP-OES, 1 mL min ⁻¹ , 1.2 kW, 0.85 L min ⁻¹	[146]
	Methanol (≈ 30 %)	≈ 30	≈ 1.7	Aerosol	ICP-MS, 0.33 mL min ⁻¹ , 1.3 kW, 1.05 L min ⁻¹	[161]
	Triethanolamine (6 %)	≈ 33	2.0	Aerosol	ICP-MS, 1 mL min ⁻¹ , 1.35 kW, 0.60 L min ⁻¹ , 8 mm	[150]
P	Acetonitrile (40 %)	≈ 190	≈ 9.3	Charge transfer	ICP-MS ³	[145]

(10.49 eV)						
------------	--	--	--	--	--	--

¹Improvement of aerosol transport efficiency. ²Charge transfer reactions from C⁺ species to analyte atoms. ³No operating conditions are provided. ⁴Minor mechanism. ⁵Added to the nebulizer gas flow rate. ⁶Not discussed.

Table 10: Compilation of selected examples resulting in signal enhancement higher than 1.1 classified according to the considered carbon sources and their amounts. Main enhancement mechanisms are indicated.

Carbon source	Carbon source content	C (g L ⁻¹)	Analytes	Signal enhancement		Ref.
				Factor	Principal source	
Acetic acid	≈ 40 %	170	As	≈ 3.1	Charge transfer ¹ + possible aerosol ²	[161]
			Hg	≈ 1.7	Possible aerosol	
			Se	≈ 3.0	Charge transfer + possible aerosol	
Acetone	≈ 0.6 %	≈ 3	Cd	≈ 1.3	Aerosol	[161]
			Rb	≈ 1.2		
	≈ 2 %	≈ 10	As	≈ 4.4	Aerosol + charge transfer	
			Hg	≈ 1.8	Aerosol	
		Se	≈ 4.4	Aerosol + charge transfer		
Acetonitrile	2 %	≈ 2	As	≈ 2.8	Ionization equilibrium modification due to C species	[142]

	20 %	≈ 90	Y	≈ 1.6	Charge transfer	[145]
	30 %	≈ 140	As	≈ 6.1		
			Ge	≈ 2.4		
			Se	≈ 7.3		
	40 %	≈ 190	P	≈ 9.3		
Ammonium carbonate	≈ 0.3 mol L ⁻¹	4	As	2.3 (As ^{III})	Charge transfer	[141]
Blood serum	/	/	Se	3	Charge transfer	[154]
Butanol	1 %	≈ 5	Se	≈ 2.5	Aerosol + charge transfer	[152]
CFA-C (amine)	10 %	/	As	2.1	/ ³	[149]
			Se	1.5 (⁷⁷ Se), 1.3 (⁸² Se)	/	
Ethanol	2 %	≈ 8	Se	≈ 3.5	Aerosol + charge transfer	[152]
Ethylenediamine	6 %	≈ 22	Hg	1.5	Aerosol	[150]
Glycerol	1 mol L ⁻¹ ≈ 7 %	≈ 36	As	2.4	Ionization equilibrium modification due to C species	[146]
			Au	3.25		
			Hg	6		
			Se	2.5		
			Te	1.9		
Glycine	≈ 6 % (m/v)	20	B	1.5	Charge transfer + carbon space	[147]
			Be	1.15		

					charge effect + (other species space charge effects) ⁴	
Glucose	$\approx 0.15 \text{ mol L}^{-1}$	10	Se	1.4	Charge transfer	[148]
Isopropanol	$\approx 0.08 \text{ mol L}^{-1}$ $\approx 0.8 \%$	≈ 2.9	Be	≈ 1.5	Aerosol + (charge transfer)	[144]
		≈ 2.9	Cu	≈ 1.5	Aerosol	
		≈ 2.9	In	≈ 1.8		
	≈ 2.9	Zn	≈ 1.8	Aerosol + possible charge transfer		
	$\approx 0.1 \text{ mol L}^{-1}$ $\approx 1 \%$	≈ 3.6	Se	≈ 2.5	Aerosol + charge transfer	
Methane⁵	4 %	≈ 20	As	≈ 5.5	Ionization	[146]
			Se	≈ 3.5	equilibrium	
			Te	≈ 3.5	modification due to C species	
Methanol	2 %	≈ 5.9	Se	≈ 3	Aerosol + charge transfer	[152]
	3 %	≈ 9	As	3.4 (As ^{III}), 4.2 (DMA), 4.5 AsB)	Aerosol + charge transfer	[141]

			Sb	1.5	Aerosol	
			Se	3.4 (Se ^{IV}), 3.1 (SeMet)	Aerosol + charge transfer	
	5 %	≈ 15	As	≈ 2.3	Ionization equilibrium modification due to C species	[142]
	≈ 5 %	≈ 15	Cd	≈ 1.4	Aerosol	
			Rb	≈ 1.2		
	≈ 10 %	≈ 30	As	≈ 3.5	Aerosol + charge transfer	[161]
			Hg	≈ 1.7	Aerosol	
			Se	≈ 3.1	Aerosol + charge transfer	
	20 %	≈ 59	As	31	Charge transfer + aerosol	[140]
			Co	17	Aerosol + possible charge transfer	
			Mg	31		
			Pb	6	Aerosol + (charge transfer)	
			Rh	12		
			Se	6	Charge transfer	

					+ aerosol	
			Y	5	Aerosol + (charge transfer)	
Propanol	1 %	≈ 5	Se	≈ 2	Aerosol + charge transfer	[152]
Sodium bicarbonate	25 mmol L ⁻¹	≈ 0.3	As	1.5	Charge transfer	[151]
			Se	1.5		
Sodium dodecylsulfate (SDS)	0.2 % m/v	≈ 1.0	Al	≈ 2	Aerosol + electrostatic effects	[120]
			As	≈ 1.5	Aerosol + electrostatic effects + charge transfer	
			Co	≈ 1.5	Aerosol + electrostatic effects	
			Cu	≈ 1.2	Aerosol + electrostatic effects	
			Ni	≈ 1.4	Aerosol + electrostatic effects	

			Sb	≈ 1.2	Aerosol + electrostatic effects + charge transfer	
			Se	≈ 1.2	Aerosol + electrostatic effects + charge transfer	
			Zn	≈ 1.4	Aerosol + electrostatic effects + charge transfer	
Triethanolamine	6 %	≈ 33	Hg	2.0	Aerosol	[150]

¹Charge transfer reactions from C⁺ species to analyte atoms. ²Improvement of aerosol transport efficiency. ³Not discussed. ⁴Minor mechanism. ⁵Added to the nebulizer gas flow rate.

Table 11: Maximum ionization efficiency in ICP-MS for hard-to-ionize elements (efficiency < 90 %) together with calculated and experimental maximum enhancement factor (experimental factors are obtained from Tables 9 and 10).

	Elements	Ionization efficiency (%) [160]	Ionization energy (eV) [167]	Calculated maximum enhancement factor	Experimental maximum enhancement factor
Ionization energy 9-11 eV	As	52	9.79	1.9	≈ 31
	Au	51	9.23	2.0	≈ 3.25
	Be	75	9.32	1.3	≈ 1.5
	Hg	38	10.44	2.6	≈ 6
	I	29	10.45	3.4	/
	P	33	10.49	3.0	≈ 9.3
	S	14	10.36	7.2	/
	Se	33	9.75	3.0	≈ 7.3
	Te	66	9.01	1.5	≈ 3.5
	Zn	75	9.39	1.3	≈ 1.8
Other elements	B	58	8.30	1.7	≈ 1.5
	Br	5	11.81	20	/
	Cd	85	8.99	1.2	≈ 1.4

	Cl	0.9	12.97	111	/
	Os	78	8.44	1.3	/
	Pt	62	8.96	1.6	/
	Sb	78	8.61	1.3	≈ 1.5
	Si	85	8.15	1.2	/